Organic Geochemistry 97 (2016) 78–94

Contents lists available at ScienceDirect

Organic Geochemistry

journal homepage: www.elsevier.com/locate/orggeochem

De-convoluting crude oil mixtures from Palaeozoic reservoirs in the Tabei Uplift, Tarim Basin, China

Zhao-Wen Zhan [a,b], Yankuan Tian [a], Yan-Rong Zou [a,*], Zewen Liao [a], Ping'an Peng [a]

[a] State Key Laboratory of Organic Geochemistry, Guangzhou Institute of Geochemistry, Chinese Academy of Sciences, Guangzhou 510640, China
[b] University of Chinese Academy of Sciences, Beijing 10039, China

ARTICLE INFO

Article history:
Received 20 January 2016
Received in revised form 19 March 2016
Accepted 1 April 2016
Available online 9 April 2016

Keywords:
Mixed oil
Alternating least square
De-convoluting
Tarim Basin

ABSTRACT

Geochemical characteristics of 61 crude oil samples collected from Palaeozoic reservoirs in the Tarim Basin (60 from the Tabei Uplift and one from the Tazhong Uplift) were analyzed. The samples proved to be mixed oils of different maturity from diverse source rocks. Concentrations of 40 biomarkers and carbon isotopic compositions for the whole oils were analyzed by alternating least squares (ALS) regression to de-convolute the mixtures. Three endmember (EM) oils were identified. EM1 is the minimum contributor to the mixed oils, accounting for less than 10% of most oils. EM1 originated from Cambrian–Lower Ordovician source rocks in the early to peak oil window stage and experienced two phases of mixing and biodegradation. EM2 is the secondary contributor with proportions ranging from 10% to 40% in most oil samples. EM2 originated from Middle–Upper Ordovician source rocks at the early oil generation stage and underwent two phases of mixing and one stage biodegradation in the reservoirs. EM3 is the major contributor to most samples with proportions ranging from 13% to 95%. EM3 was generated from Middle–Upper Ordovician source rocks at the late oil generation stage and mixed with earlier emplaced mixtures in the reservoirs. The final mixtures that were not biodegraded are currently exploited from Palaeozoic reservoirs in the Tabei Uplift. Biomarkers in the crude oils reveal mixed characteristics, including evidence for two phases of oil charge and severe biodegradation.

1. Introduction

The Tarim Basin is a typical superimposed basin. It consists of a Paleozoic cratonic basin overlain by Mesozoic–Cenozoic foreland depressions (Li et al., 1996) and is one of the most important petroleum basins in China. There are two main characteristics of petroleum systems in complex petroliferous basins. First, such basins are characterized by multiple reservoirs that are widely distributed both horizontally and vertically. The occurrence and formation of marine oils and reservoir bitumen in the Tarim Basin attracted attention in the past decade due to the long, complex and deep burial history of hydrocarbons (Hanson et al., 2000; Li et al., 2000, 2010; Zhang et al., 2000, 2004, 2005; Sun et al., 2003; Zhang and Huang, 2005; Jia et al., 2008, 2010; Cai et al., 2009a,b; Pan and Liu, 2009; Yu et al., 2011). Second, such basins contain a range of petroleum types, including dry gas, wet gas, condensate, light oil, heavy oil and solid bitumen. Multiple oil generation and filling stages and a number of post-accumulation processes, *e.g.*, mixing, biodegradation, fractionation, have been proposed to explain the diverse oil occurrence and formation (Zhang, 2000; Wang et al., 2008; Pan and Liu, 2009; Jia et al., 2010, 2013; Zhang et al., 2011, 2014, 2015; Li et al., 2012, 2015; Tian et al. 2012a,b; Zhu et al., 2012, 2013, 2014b).

Although many studies have been carried out on the Tarim Basin, understanding of the oil source, maturity, and oil mixing remains limited, partly because few source rocks have been encountered by exploration (Jia et al., 2013). Cambrian–Lower Ordovician and Middle–Upper Ordovician marine rocks are considered to be the sources for oil in Palaeozoic reservoirs (Liang et al., 2000; Zhang et al., 2000). Sun et al. (2003) concluded that crude oil in the Tarim Basin mainly originated from the Cambrian–Lower Ordovician source rocks based on aryl isoprenoid distributions. Zhang et al. (2000, 2005) concluded that oil in Ordovician-Triassic reservoirs in the Tarim Basin had similar biomarker characteristics and was generated from Middle–Upper Ordovician source rocks. A similar conclusion was drawn by Hanson et al. (2000). An increasing number of studies suggest that marine oils from Palaeozoic reservoirs are actually mixtures generated from two marine source rocks (Li et al., 2010, 2015; Yu et al., 2011; Zhu et al., 2012, 2013,2014b; Tian et al., 2012b ; Tian, 2013). However, it remains unclear what proportions of those two sources

* Corresponding author. Tel.: +86 20 85290187; fax: +86 20 85290706.
E-mail address: zouyr@gig.ac.cn (Y.-R. Zou).

http://dx.doi.org/10.1016/j.orggeochem.2016.04.004
0146-6380/

contribute to the oils and when and how the mixing process occurred. Li et al. (2010, 2015) showed that the majority of oils in the Tazhong Uplift are mixtures derived from two source rocks and calculated the percentage contributions of the Cambrian–Lower Ordovician ranging from 19% to 100% by combining carbon isotopic compositions and concentrations of *n*-alkanes (averaged $\delta^{13}C$ values and concentrations of *n*-C_{11} to *n*-C_{25}) in oil based on the assumption of two assigned endmember oils. Tao et al. (2010) estimated the relative contributions of these two source rocks to the oils in the Ordovician reservoir in Tahe oilfield by multivariate data analysis using quantitative data from tricyclic terpanes and hopanes. Assigning two endmember oils in a series of samples, the contribution of the Cambrian–Lower Ordovician source rocks to oils in Tabei Uplift was estimated on the basis of the concentrations of normal alkanes and 25-norhopanes (Yang et al., 2003) and C_{28} 5α,14α,17α(H)-ergostane 20R (C_{28}ααα R) and triaromatic steroids (Tian, 2013).

It is difficult to identify and evaluate quantitatively the relative contribution from each candidate source rock to mixed oil in basins with multiple source rocks and episodic charge histories, particularly when petroleum from several different source rocks have mixed in the same reservoir (Arouri and McKirdy, 2005). The purpose of this study is to de-convolute the crude oils from the Tabei Uplift in the Tarim Basin. This work aims to determine the number of endmember oils, calculate the relative contributions of each endmember, predict the compound compositions of endmember oils, and discuss relevant issues and geological interpretations.

2. Geological setting

The Tabei Uplift is situated between the Manjar Depression to the south and the Kuqa Depression to the north (Fig. 1). It is a long-lived structural high developed on pre-Sinian basement metamorphic rock, with marine depositional sequences from the Cambrian to the Devonian, interbedded with marine and terrigenous sequences from the Carboniferous to the Permian and terrigenous sedimentation from the Triassic to the Quaternary (Zhu et al., 2013). It comprises the Yingmaili Low Uplift, the Halahatang Depression, the Lunnan Low Uplift, the Caohu Depression, and other secondary structures from west to east (Fig. 1c). The Tabei Uplift was a large northeast trending structural nose in the middle–late Caledonian period, and reformed in the early Hercynian orogeny. During long term uplift and exposure, the Silurian–Devonian and Middle–Upper Ordovician strata were partially eroded. In the Yanshan-Himalayan period, the Tabei area dipped toward the north to form the present structure (Zhu et al., 2013). The Lunnan Low Uplift formed in the late Caledonian to early Hercynian and

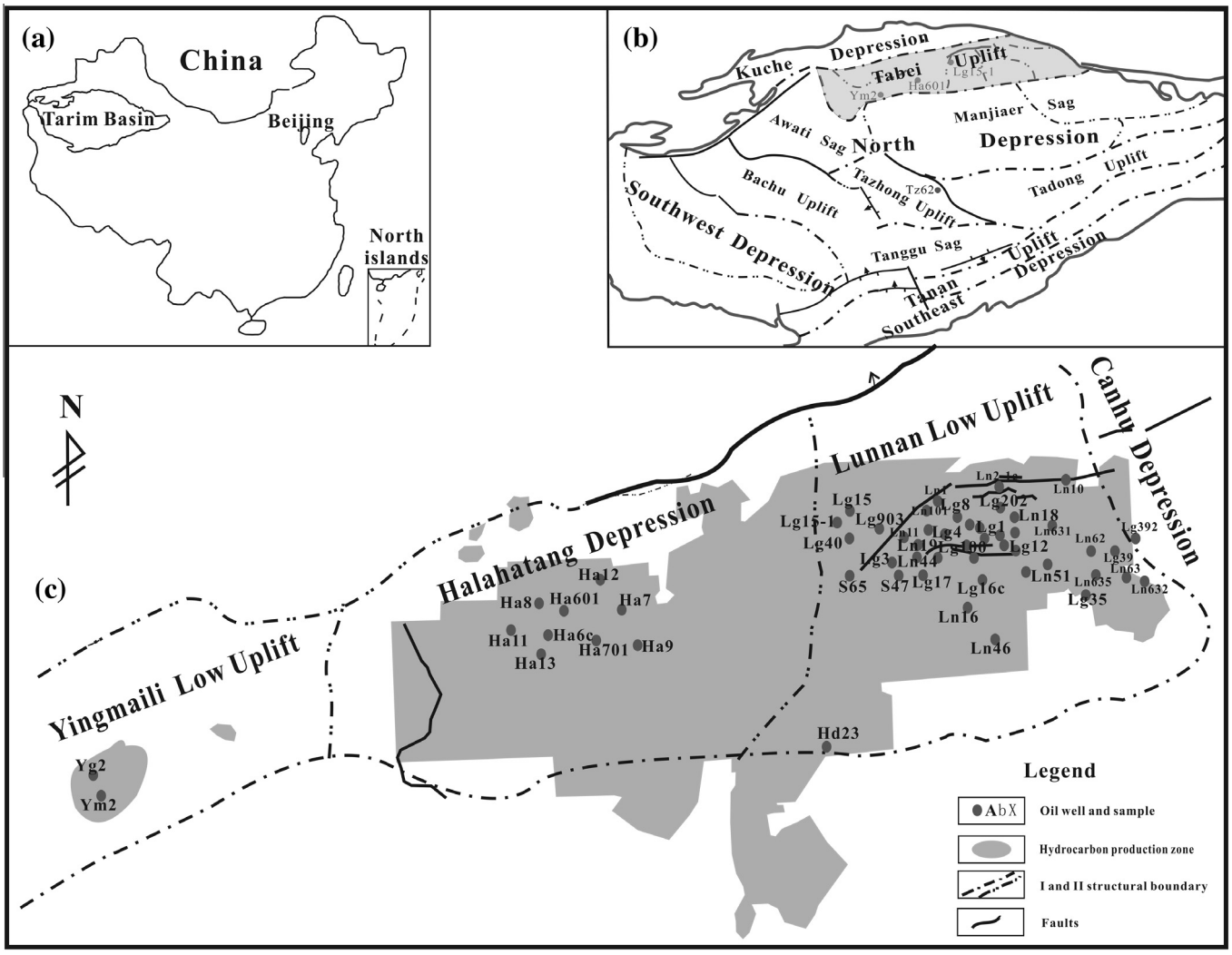

Fig. 1. Study area and sample distribution. (a) Location of the Tarim Basin in China, (b) structural unit division of the basin and (c) schematic map of the Tabei Uplift showing the sample locations.

stabilized in the Indo-China to Himalayan period. This area can be divided into five units: the Lungu eastern, the Lunnan fault horst, the central slope, the Sangtamu fault horst and the Lungu western.

Hydrocarbons in the Tabei area are known to be derived from marine Cambrian–Lower Ordovician and Middle–Upper Ordovician source rocks. The former were deposited in evaporative lagoons and starved basins under strongly reducing conditions throughout most of the cratonic region of the Tarim Basin and are generally overmature (>2.0 %Ro, Zhang et al., 2004). The latter consist mainly of argillaceous limestones and marlstones deposited in shelf edge and slope environments and are mature to overmature with respect to oil generation (Ro 0.8–1.5%, Hanson et al., 2000; Zhang et al., 2000; Zhang and Huang, 2005). The two end members have significant differences in their biomarker compositions. The Cambrian–Lower Ordovician source rocks are characterized by abundant C_{28} steranes, gammacerane, dinosterane and triaromatic steroids, 4-methyl steranes, C_{26}-norcholestane, tricyclic terpanes, with a low content of diasteranes and heavy $\delta^{13}C$ values of individual *n*-alkanes for related oils. The Middle–Upper Ordovician source rocks have the opposite characteristics (Zhang et al., 2000, 2004, 2005).

The Lower Ordovician is primarily comprised of platform dolomite and argillaceous limestone, whereas the Middle–Upper Ordovician mainly consists of platform and marginal slope-shelf carbonate sediments. The Ordovician strata can be subdivided into six formations, which are, from bottom to top, the Penglaiba (O_1p), Yingshan ($O_{1\text{-}2}y$), Yijianfang (O_2yj), Qiaerbake (O_3q), Lianglitage (O_3l) and Sangtamu (O_3s) formations. Karst reservoirs are well developed in the Ordovician sequence of the Tabei Uplift, occurring in the Yingshan ($O_{1\text{-}2}y$) and Yijianfang formations (O_2y). The seal rocks are tight muddy limestone and mudstone of the Upper Ordovician Lianglitage (O_3l) and Sangtamu formations (O_3s); while in the structural high point of the uplift where the Ordovician sequences are absent, tight siltstone of the Silurian Kepingtage Formation (S_1k) or Carboniferous mudstone can act as effective seal rocks.

3. Samples and methods

3.1. Sample distributions

There are different types of crude oil in the Tabei Uplift, which contain the largest proven oil/gas reserves in the basin, including the giant Tahe, Lunnan and Yingmaili oilfields. Light oil is mainly produced in the eastern region, whereas heavy oil can be found throughout the area. In order to facilitate the quantitative analysis of biomarkers, light oil or condensate samples were excluded from this study. Sixty crude oil samples were collected from the Lunnan Low Uplift, Halahatang Depression, and Yingmaili Low Uplift. These oils were recovered from Palaeozoic reservoirs, including Ordovician and Carboniferous, and their locations are shown in Fig. 1. The Tz62 Silurian oil (sample 61 from the Tazhong Uplift) that was identified as the endmember oil generated from the Cambrian–Lower Ordovician source rocks (Li et al., 2010, 2015; Tian et al., 2012b; Tian, 2013) was added to the sample set to meet the needs of geological interpretation.

3.2. Experiments

3.2.1. GC analysis

A measured volume of *n*-hexane was added to about 10 mg of oil sample with the internal standards of *n*-$C_{15}D_{32}$, *n*-$C_{20}D_{42}$ and *n*-$C_{24}D_{50}$ to quantify normal alkanes. The mixture was allowed to stand for more than one night, and the supernatant was analyzed using a Thermo Finnigan Trace Gas chromatograph equipped with an FID. An HP-5MS capillary column (60 m, 0.32 mm i.d., 0.25 μm film thickness) was used with nitrogen as the carrier gas (constant current mode, current speed 1.0 mL/min). The initial GC oven temperature was 35 °C, which was held for 2 min and then programmed to 295 °C at 3 °C/min, then held isothermally for 20 min.

3.2.2. Carbon isotopic analysis of whole oil

Around 1 mg oil wrapped in a tin boat was put in the autosampler of a Thermo Finnigan-Delta XL stable isotope ratio mass spectrometer. The temperatures for oxidation and reduction tubes were set at 950 °C and 650 °C, respectively. The CO_2 reference gas was calibrated against the NBS-22 oil standard, and a working standard (black carbon) was measured to monitor the system. The $\delta^{13}C$ value was reported relative to VPDB. Each sample was measured at least two times until the error was <0.5‰. The average for the two runs was accepted as the final sample carbon isotopic result.

3.2.3. Oil fractionation

Excess *n*-hexane was added to the crude oil of known quantity, then mixed ultrasonically and centrifuged at 3500 rpm to remove asphaltenes. The supernatant solution was extracted and concentrated to about 1 mL. Column chromatography was completed on the concentrates using activated silica gel/alumina columns (3:1 v:v) to fractionate saturated hydrocarbons, aromatic hydrocarbons and a polar fraction by sequential elution with *n*-hexane, toluene and ethanol. Each group was weighed to calculate their percentage in the oil.

3.2.4. GCMS analysis

For quantitative determination of aliphatic and aromatic hydrocarbons, known concentrations and amounts of the standard compounds 2,2,4,4-d4-5α,14α,17α-20R-cholestane and d8-dibenzothiophene were added to the saturated and aromatic hydrocarbons, respectively. The GCMS analyses of the saturate and aromatic fractions with internal standards were performed by means of a DSQ II MS detector combined with Thermo Fisher Trace GC Ultra analyzer. The GC used a DB-1 MS capillary column (60 m, 0.32 mm i.d., 0.25 μm film thickness) with helium as carrier gas (1.2 mL/min). For saturates, the GC oven temperature was initially set at 80 °C for 4 min and then programmed to 290 °C at 4 °C/min, holding isothermally for 15–25 min. For aromatics, the temperature was initially set at 80 °C for 4 min and then programmed to 290 °C at 3 °C/min, holding isothermally for 15 min. The MS operated in electron impact (EI) ionization mode at an electron energy of 70 eV and ion source temperature of 260 °C. The analysis was conducted using mode-combining selective ion monitoring (SIM) with full-scan detection in the scan range from 50 to 650 Da. For the saturate fraction, selected ions included *m*/*z* 191, 217, 218 and 221; and for the aromatic fraction selected ions included *m*/*z* 192 and 231.

3.3. Methods

3.3.1. ALS-C de-convoluting

Chemometrics uses multivariate statistics to recognize patterns and extract useful information from measured data. Compared with univariate or bivariate techniques, which only deal with one or two variables at a time, multivariate techniques treat all of the data simultaneously using matrix algebra, and describe a sample by a point in space that has as many axes as variables (Peters et al., 2005), which allows more comprehensive and in-depth understanding of geological samples. Applications of chemometrics in petroleum geochemistry have been reported and summarized (Peters et al., 2005, 2007, 2008a,b, 2013, and references therein). Alternating least squares of biomarker concentrations (ALS-C), a kind of multivariate statistical or chemometrics method,

provides an excellent way to calculate the number, proportions, and compound compositions of the endmembers in mixed oil samples. The principles of the method to de-convolute mixed oils were discussed and summarized in detail by Peters et al. (2008b) and Zhan et al. (2016). In this study, ALS from Pirouette® software version 4.5 (Infometrix, Inc.) was employed to de-convolute mixed oils from the Tabei Uplift in the Tarim Basin, NW China. In ALS, maximum sources were designated as three, which will be discussed later. Rows were chosen to produce the initial estimates. Some constraints include non-negativity of amounts and profiles and closure of amounts. Principal component analysis (PCA) was used to display the distribution of the oil samples in multidimensional space. PCA (Pirouette) settings: preprocessing = autoscale, maximum factors = 10, validation method = none, and row = none.

3.3.2. Datasets

Identifications of biomarkers and polycyclic aromatic hydrocarbons (PAHs) were performed by comparison with reference mass spectra from previous studies. The concentrations of individual compounds, including biomarkers and PAHs, were calculated according to the corresponding internal standard concentration based on peak areas. Relative response factors (RRF) for each target compound versus the internal standard were assumed to be 1. In this study, a dataset consisting of 40 biomarker concentrations and the carbon isotopic ratios of the whole oils (Tables 3 and 4) was used in the chemometric analysis. Because the concentrations of different biomarkers in the same oil sample and the concentrations of the same biomarker in different oil samples vary considerably, rescaling of the data is necessary. Concentration normalization of the same biomarker in all oils is used to ensure that the data are consistent. The formula for concentration normalization is $C_{NB\text{-}r} = (C_{NB\text{-}i} - C_{B\text{-}min})/(C_{B\text{-}max} - C_{B\text{-}min})$. The $C_{NB\text{-}r}$ and $C_{NB\text{-}i}$ respectively refer to the values after and before normalization of biomarker B (includes absolute value of whole oil $\delta^{13}C$) in oil N. The $C_{B\text{-}max}$ and $C_{B\text{-}min}$ are, respectively, the maximum and the minimum of biomarker B concentration before normalization of all oil samples. Each parameter in all oils ranges from 0 to 1 in the new dataset, which consists of normalized concentrations for 40 biomarkers and the whole oil carbon isotopic ratios. Since ALS cannot handle negative numbers, the $\delta^{13}C$ values were taken as their absolute positive value and then normalized. The new dataset is also called the concentration dataset (C) in Appendix 1. The biomarker concentrations of endmember oils calculated from ALS-C need to be transformed into the original concentrations using on the formula of $C_{B\text{-}EM} = C_{BA\text{-}EM} \times (C_{B\text{-}max} - C_{B\text{-}min}) + C_{B\text{-}min}$. The $C_{B\text{-}EM}$ and $C_{BA\text{-}EM}$, respectively, denote the concentration and the value calculated by ALS-C of biomarker B in the endmember oil.

3.3.3. Repeatability

Repeatability of the ALS-C analyses was examined by comparing predicted relative contributions from each endmember (EM) to oil samples produced from the same well. For example, for two samples in the Ln19 well, sample 34 from 5570–5585 m and sample 35 from 5338–5360 m, the relative contributions of EM1, EM2 and EM3 calculated by ALS-C are 8:11:81 and 10:9:81, respectively. Different relative contributions of endmembers to oil samples from different depths indicate a variable mixing ratio.

4. Results and discussion

4.1. Geochemical characteristics of the oils

4.1.1. Carbon isotope and group compositions

The stable carbon isotope ratio ($\delta^{13}C$) of crude oil mainly depends on the depositional environment and organic input of source rocks, and is not significantly influenced by geochemical alteration after accumulation. The whole oil $\delta^{13}C$ of oil samples from Palaeozoic reservoirs in the Tabei Uplift show relatively small variations, between −31.31‰ and −33.76‰, with an average of −32.17‰. Subtle variations exist in the transect from west to east (Table 3). The whole oil $\delta^{13}C$ values for the samples indicate similar marine source rocks and local variations are attributed to slight differences in maturity and/or source rock organic facies.

Unlike the carbon isotopic ratio, the bulk compositions of the oils vary significantly (Table 1). These oils contain prominent saturated hydrocarbons (10.6–87.9%, average of 58.0%), with relatively low aromatic hydrocarbons (3.0–23.7%, average of 12.6%) and resins + asphaltenes (7.4–82.8%, average of 29.1%). The ratios of total saturated to aromatic hydrocarbons fall in the range from 1.0 to 18.9. There is no systematic change in bulk group compositions along the transect and with reservoir depth, indicating the complexity of petroleum accumulation in the Tabei Uplift.

4.1.2. GC of whole oils

n-Alkanes and isoprenoids are commonly used in petroleum geochemistry, but are readily altered by geochemical processes, such as biodegradation. In recharged mixtures after severe biodegradation, the *n*-alkanes and isoprenoids are in many cases solely derived from late charge and their relative abundances may bear clues about source rock type, depositional environment, and maturity (Zhang et al., 2005).

The distributions of *n*-alkanes and isoprenoids are displayed in gas chromatograms (GC) of the whole oils. Complete *n*-alkanes (*n*-C_9 to *n*-C_{30+}) and isoprenoids (*i*-C_{13} to *i*-C_{20}) were detected in all of the crude oil samples and yet almost every GC trace also showed a significant unresolved complex mixture (UCM). Despite these similarities, there are also differences in the distribution patterns carbon numbers of the main peaks, relative abundances of low to high molecular-weight *n*-alkanes, and size of UCM amongst the oils (Fig. 2). The total *n*-alkane concentrations ($\sum n$-C) range from 10.8 mg/g to 324 mg/g oil and the abundance ratio of low to high molecular-weight *n*-alkanes ($\sum n$-$C_{21-}/\sum n$-C_{22+}) ranges from 0.61 to 9.85 (Table 1). Such large differences within the same reservoir unit suggest complex processes, such as biodegradation, mixing, and fractionation during or after hydrocarbon accumulation.

Ratios of pristane to phytane (Pr/Ph) range from in 0.74 to 1.20 with an average of 0.98. Pr/*n*-C_{17} and Ph/*n*-C_{18} range from 0.06 to 0.61 and 0.02 to 0.67 (Table 1), respectively. A good positive relationship exists between them and all oils plot in a region designated for algal kerogens (Connan and Cassau, 1980; figure is not shown).

4.1.3. Biomarker composition and distribution

Fig. 3 shows examples of terpane biomarker distributions for some typical samples from the study area. Selected geochemical parameters are summarized in Table 2. Tricyclic terpanes (TT) with carbon numbers from C_{19} to C_{29} (C_{19}TT to C_{29}TT) occur in all of the oil samples, with C_{23}TT being the main peak. The ratios of C_{19}TT/C_{23}TT and C_{21}TT/C_{23}TT range from 0.05 to 0.48 and 0.34 to 0.69, with averages of 0.22 and 0.48, respectively. C_{24} tetracyclic terpane (C_{24}Te) is also detected at comparable or slightly higher relative intensity compared with C_{26}TT. Ratios of C_{24}Te/ C_{26}TT range from 0.49 to 1.15 and average 0.77. Except for seven oil samples, most samples have higher relative abundances of long-chain (C_{26}TT to C_{29}TT) than short-chain tricyclic terpanes (C_{19}TT to C_{21}TT) with their ratio ($\sum C_{19-21}$TT/$\sum C_{26-29}$TT) less than 1.0 (Table 2). Pentacyclic terpanes in most samples are dominated by C_{29} and C_{30} hopanes (C_{29}H and C_{30}H), and the relative intensities of homohopanes (C_{31}H–C_{35}H) generally decrease with increasing carbon number. However, the relative abundances of some biomarkers vary, indicating differences in origin, or secondary processes

Table 1
Basic information, group compositions, and paraffinic hydrocarbon parameters of the oil samples.

No.	Well	Reservoir	Depth/m	Sat./%	Aro./%	Res. + Asp./%	Sat./Aro.	Pr/Ph	Pr/nC_{17}	Ph/nC_{18}	$\sum n$-C_{21}-/$\sum n$-C_{22}+	$\sum n$C, mg/g
1	Ln632	O	6452–6472	75	9	16	8.3	0.74	0.36	0.52	2.55	158.38
2	Lg392	O	6330–6350	70	14	17	5.1	0.81	0.36	0.52	4.21	135.49
3	Lg39	O	5861–5717	64	7	30	9.5	0.99	0.28	0.32	9.85	216.27
4	Lg352	O	5872–6110	75	10	15	7.4	0.99	0.22	0.22	1.04	147.88
5	Ln62	C	5565–5578	64	16	20	3.9	0.94	0.32	0.44	4.13	97.77
6	Ln635	O	5815–5842	72	10	17	7.0	0.96	0.31	0.35	2.44	171.11
7	Ln631(1)	O	5844–5884	79	11	10	7.0	0.78	0.22	0.25	1.06	152.02
8	Ln631(3)	O	5902–5990	74	11	15	6.9	0.93	0.23	0.23	0.61	124.93
9	Ln63(2)	O	5957–6071	53	10	37	5.3	0.86	0.31	0.42	2.68	84.31
10	Lg100-H1	O	5541–5605	64	11	26	6.0	1.06	0.33	0.36	2.93	185.42
11	Lg100	O	5431–5525	70	15	15	4.8	1.00	0.29	0.31	1.90	150.91
12	Lg101-4	O	5459–5490	71	12	17	5.8	1.10	0.29	0.29	1.69	161.85
13	Lg12	O	5407–5528	46	19	35	2.4	1.01	0.29	0.34	6.37	133.67
14	Lg16c	O	5468–5600	71	10	19	7.4	0.96	0.28	0.30	1.71	147.84
15	Lg17C	C	5245–5268	56	3	41	18.5	1.20	0.23	0.25	9.85	324.92
16	Lg17(o)	O	5464–5479	68	13	19	5.2	0.95	0.28	0.32	2.12	161.46
17	Ln51	O	5418–5550	67	16	18	4.3	0.95	0.35	0.40	1.56	159.72
18	Ln44	O	5283–5323	66	6	28	11.3	1.01	0.32	0.39	5.50	230.05
19	Ln46	O	6119–6144	65	10	25	6.3	1.09	0.35	0.40	3.29	162.80
20	Ln16	O	5585–5605	74	10	16	7.7	0.95	0.61	0.61	2.34	137.55
21	Lg4O1	O	5270–5296	58	15	27	3.9	1.00	0.25	0.31	4.80	116.64
22	Lg4O	O	5379–5397	64	9	27	7.6	1.00	0.33	0.36	2.76	184.20
23	Lg8	O	5145–5220	67	11	22	6.1	0.98	0.30	0.34	2.34	182.55
24	Ln8	O	5167–5230	71	12	16	5.7	0.92	0.22	0.25	1.87	160.33
25	Lg1	O	5210–5590	69	5	26	13.3	1.05	0.24	0.25	2.86	238.27
26	Lg202	O	5142–5146	67	8	25	8.2	1.07	0.31	0.35	3.06	217.13
27	Lg208	O	5330–5370	71	12	17	5.7	1.00	0.25	0.28	2.71	175.70
28	Ln18-1	O	5244–5350	54	13	33	4.0	0.95	0.36	0.46	3.77	118.52
29	Lg6c	O	5416–5430	69	8	23	8.7	1.17	0.27	0.28	3.43	207.33
30	Lg2-1	O	5421–5510	65	13	22	5.1	1.09	0.35	0.35	2.56	126.84
31	Lg2	O	5345–5431	63	16	21	4.1	1.07	0.35	0.37	2.34	139.70
32	Lg21	O	5043–5060	75	5	20	14.5	0.95	0.26	0.29	2.00	181.82
33	Lg201	O	5350–5353	67	13	20	5.1	1.03	0.28	0.30	2.61	164.92
34	Ln19(1)	O	5570–5585	53	17	31	3.2	0.95	0.36	0.45	3.93	147.62
35	Ln19(2)	O	5338–5360	54	18	27	3.0	0.96	0.34	0.39	4.07	144.25
36	Ln10(1)	O	5283–5343	65	4	31	15.5	1.04	0.36	0.44	5.30	200.82
37	Ln2-1c	O	5364–5458	64	14	22	4.5	1.17	0.37	0.36	2.39	127.35
38	Ln11	O	5278–5310	11	6	83	1.7	1.05	0.06	0.02	1.07	10.79
39	Lg3	C	5196–5270	58	11	30	5.1	1.15	0.39	0.38	5.01	201.57
40	Ln101	O	5049–5150	88	5	7	18.9	1.00	0.39	0.45	7.43	243.96
41	Ln1	O	5038–5052	31	17	52	1.8	0.93	0.37	0.48	3.85	71.87
42	Lg15	O	5726–5750	35	16	49	2.3	0.90	0.37	0.49	4.73	101.21
43	Lg15-1	O	5904–5954	11	7	82	1.5	0.87	0.32	0.43	5.59	73.72
44	Lg40	O	5339–5346	45	17	38	2.6	0.91	0.39	0.53	4.89	86.54
45	Lg903	O	5530–5568	13	12	76	1.1	0.90	0.13	0.17	2.35	11.65
46	S47	O	5344–5370	/	/	/	/	0.85	0.36	0.50	4.88	/
47	S65	O	/	29	29	42	1.0	0.95	0.41	0.52	5.68	/
48	Ha6c(1)	O	6731–6830	60	23	17	2.6	0.83	0.41	0.59	4.56	77.96
49	Ha6c(2)	O	6746–6830	49	17	34	2.8	1.06	0.49	0.57	6.86	78.19
50	Ha7	O	6622–6646	48	19	32	2.5	1.02	0.37	0.41	5.31	104.58
51	Ha8	O	6643–6680	48	15	37	3.2	0.97	0.35	0.43	8.70	149.58
52	Ha9	O	6598–6710	37	19	44	1.9	0.97	0.58	0.67	6.48	49.19
53	Ha11	O	6658–6748	60	16	24	3.6	1.10	0.37	0.39	8.13	169.11
54	Ha12	O	6694–6696	67	21	12	3.1	1.06	0.31	0.34	8.90	192.11
55	Ha13	O	6668–6800	65	14	21	4.7	1.04	0.35	0.38	7.62	205.65
56	Ha601	O	6598–6677	26	11	62	2.4	0.95	0.32	0.38	2.78	32.98
57	Ha701	O	6557–6618	49	24	27	2.1	0.90	0.39	0.47	6.91	49.27
58	HD23	O	6253–6440	52	13	35	3.9	0.80	0.47	0.66	4.13	149.04
59	YM2	O	5940–5953	49	19	32	2.6	0.91	0.35	0.46	4.23	105.10
60	YG2	O	6009–6070	46	24	30	1.9	0.92	0.41	0.50	9.32	/
61	Tz62	S	4052–4074	44	12	44	3.6	1.16	0.44	0.41	5.52	112.76

Note: Samples 1–47 collected from the Lunnan Low Uplift; samples 48–57 from the Halahatang Depression; samples 59 and 60 from the Yingmaili Low Uplift; sample 61 (Tz62, S) from the Tazhong Uplift. O, Ordovician; C, Carboniferous; S, Silurian. Sat., saturate; Aro., aromatic; Res. + Asp., resin + asphaltene. Pr, pristane; Ph, phytane; $\sum n$-C_{21}−, the sum of low molecular-weight *n*-alkanes; $\sum n$-C_{22}+, the sum of high molecular-weight *n*-alkanes; $\sum n$C, total *n*-alkane concentration.

affecting the oils. For example, $C_{29}H/C_{30}H$ varies from 0.45 to 1.57 (Table 2). Gammacerane (G) and C_{29} 25-norhopane (25-NH) were detected almost in all samples. $G/C_{30}H$ is generally less than 0.10, with a few exceptions where the concentration is relatively high. The C_{29} 25-norhopane to $C_{30}H$ ratios (25-NH/$C_{30}H$) vary from 0.01 to 1.75 (Table 2). 17α(H)-Trinorhopane (Tm) and 18α(H)-trinorneohopane (Ts) show varied concentrations and low relative abundances, and the Ts/(Ts + Tm) ratios vary from 0.32 to 0.86 (Tables 2 and 4).

Two types of terpane distribution patterns can be identified. The first type is characterized by higher concentrations of tricyclic to pentacyclic terpanes, with the main peak at C_{23}TT and little or no hopane series in the *m*/*z* 191 fragmentogram. Ratios of $C_{23}TT/C_{30}H$ are more than 1.0 (Fig. 3, Tables 2 and 4). The second type

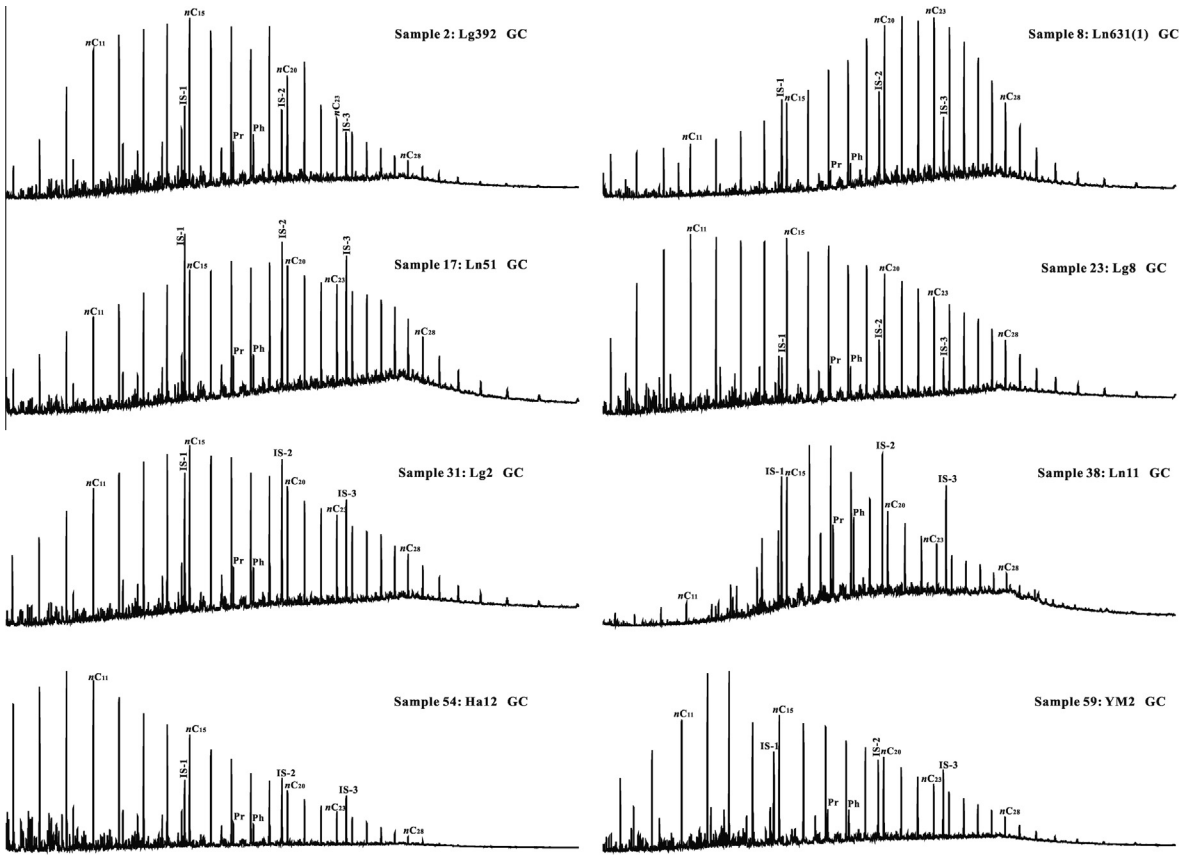

Fig. 2. Gas chromatograms (GC) of whole oil for representative samples showing *n*-alkane and isoprenoid alkane distributions. Pr, pristane; Ph, phytane; IS-1, IS-2 and IS-3 are *n*-$C_{15}D_{32}$, *n*-$C_{20}D_{42}$ and *n*-$C_{24}D_{50}$ internal standards, respectively.

shows the opposite characteristics (Fig. 3, Tables 2 and 4), with the main peak at $C_{29}H$ or $C_{30}H$ and relatively high abundance for the complete hopane series. These differences suggest different source rocks or degrees of secondary alteration, such as biodegradation, thermal maturation, and mixing.

The *m*/*z* 217 fragmentograms of saturated hydrocarbons show the sterane distributions for several samples in Fig. 3. Although the concentrations exhibit large variations (Table 3), the distributions of steranes are complete, including pregnanes, diasteranes and regular steranes. The regular steranes are characterized by a predominance of C_{29} relative to C_{28} and C_{27}. The normalized relative abundance of C_{27} steranes ($\sum C_{27}St$) are in the range from 0.22–0.36, C_{28} steranes ($\sum C_{28}St$) from 0.16–0.27 and C_{29} steranes ($\sum C_{29}St$) from 0.44–0.59 (Table 2). Two commonly used maturity parameters based on C_{29} steranes, the ratios of 20S/(S + R) and ββ/(ββ + αα), are within the ranges 0.45–0.57 and 0.47–0.64 in the studied oils (Table 2), respectively. The endpoints are 0.52–0.55 for the former and 0.67–0.71 for the latter (Peters et al., 2005), suggesting that some of the investigated oils were generated in the early to peak oil window (Fig. 5a). The relative abundances of pregnanes and diasteranes show a wide difference with regular steranes. In some oil samples, the C_{20} pregnane is the main peak in the *m*/*z* 217 fragmentogram. The ratios of C_{21-22} pregnanes to C_{27-C29} regular steranes ($\sum$preg/$\sum$reg) and C_{27} diasteranes to regular steranes (diaC_{27}/regC_{27}) vary from 0.06 to 0.33 and 0.20 to 0.58 (Table 2), respectively. The pregnanes and diasteranes are more resistant to thermal maturity and biodegradation than regular steranes. Therefore, the changes of their relative abundances may imply differences in thermal maturity or the degree of biodegradation.

4.1.4. Aromatic hydrocarbons

Aromatic hydrocarbons resist biodegradation and are an important tool to assess thermal maturity and source rock depositional environment, particularly for biodegraded oil. The distributions of phenanthrenes, methylphenanthrenes, dibenzothiophenes, methyl dibenzothiophenes and triaromatic steroid hydrocarbons are shown in *m*/*z* 178 + 192, 184 + 198 and 231 (some typical samples are in Fig. 4). Their distributions, relative abundances and concentrations are very different. The ratio of dibenzothiophenes to phenanthrene (DBT/P) relates to source rock depositional environment (Hughes et al., 1995) and is less than 1.0, except for two samples (samples 52 and 57, Table 2). Three aromatic maturity parameters, methylphenanthrene index (MPI 1, Radke and Welte, 1983), methyldibenzothiophene ratio (MDR, Radke et al., 1986) and triaromatic steroid ratio [(TA(I)/TA(I + II), Peters et al., 2005)], range from 0.53 to 0.98, 2.13 to 11.49 and 0.05 to 0.78 (Table 2), respectively, indicating the oils from the Tabei Uplift have different thermal maturities or are mixtures of oils having different maturities.

4.2. Geochemical evidences of mixed oil

4.2.1. Special compounds and GC fingerprints

The formation of 25-norhopanes (25-NHs) during extensive biodegradation is well documented in the literature (Peters et al., 2005, and references therein). When the entire 25-norhopane series occurs in a crude oil, their occurrence can be explained by microbial demethylation of hopanes (Peters and Moldowan, 1991; Peters et al., 1996). 25-Norhopanes, mainly including C_{29}- and C_{28}-norhopanes, are identified in most oils from the Tabei

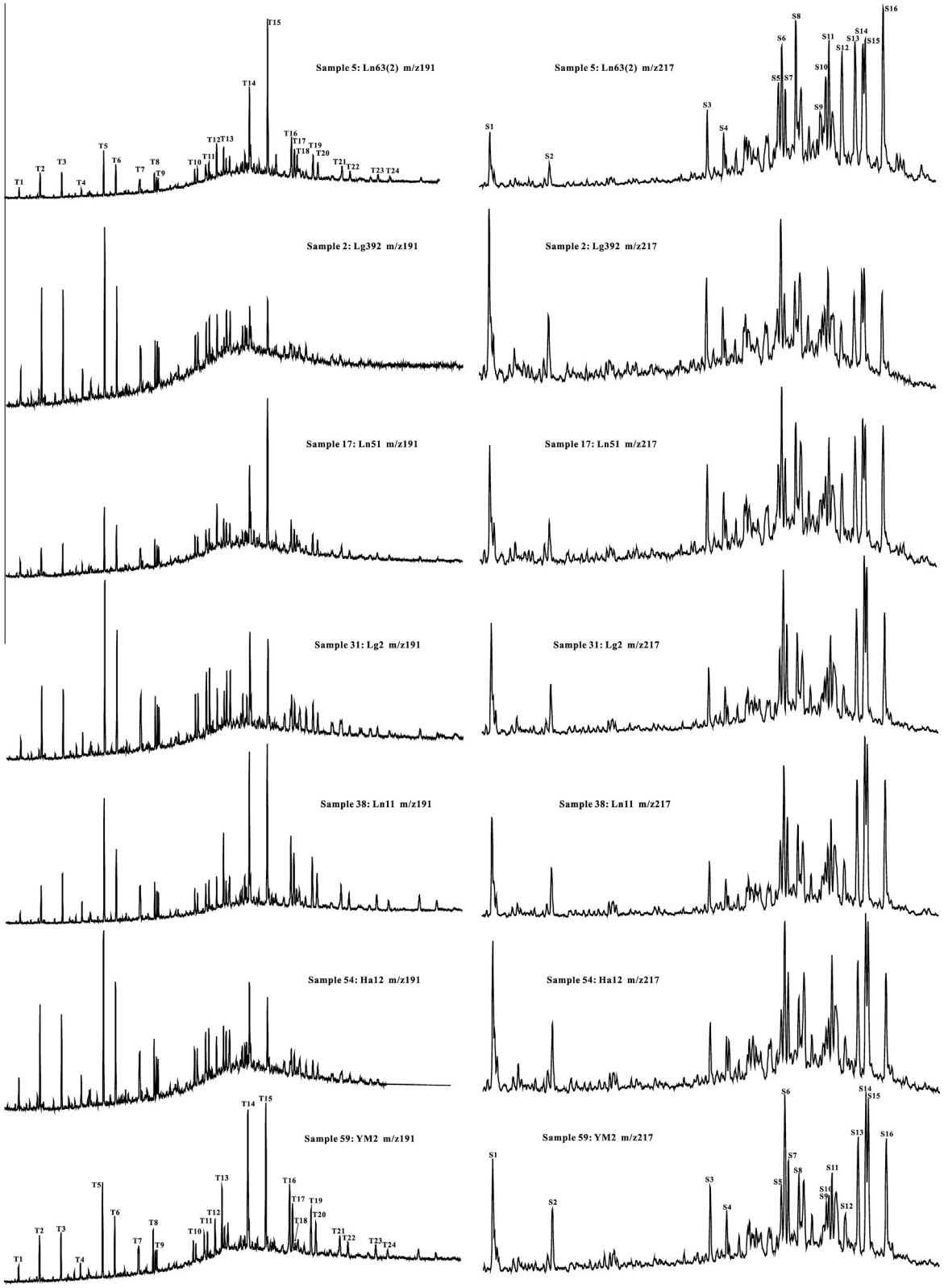

Fig. 3. Representative *m*/*z* 191 (left) and *m*/*z* 217 (right) mass fragmentograms showing the terpane and sterane distributions, respectively. *Note:* T1–T7, C_{19}–C_{25} tricyclic terpane (TT); T8, C_{24} tetracyclic terpane (C_{24}Te); T9–T11, C_{26}, C_{28}, C_{29} tricyclic terpane (TT); T12, 18α(H),21β-22,29,30-trinorneohopane (Ts); T13, 17α(H),21β-22,29,30-trinorhopane (Tm); T14, C_{29} hopane (C_{29}H); T15, C_{30} hopane (C_{30}H); T16, C_{31} homohopane 22S; T17, C_{31} homohopane 22R; T18, gammacerane (G); T19, C_{32} bishomohopane 22S; T20, C_{32} bishomohopane 22R; T21, C_{33} trishomohopane 22S; T22, C_{33} trishomohopane 22R; T23, C_{34} tetrakishomohopane 22S; T24, C_{34} tetrakishomohopane 22R; S1–S2, C_{21}–C_{22} 5α,14α,17α(H)-pregnane (preg); S3, C_{27} 13β,17α(H)-diacholestane 20S; S4, C_{27} 13β,17α(H)-diacholestane 20R; S5, C_{27} 5α,14α,17α(H)-cholestane 20S; S6, C_{27} 5α,14β,17β(H)-cholestane 20R; S7, C_{27} 5α,14β,17β(H)-cholestane 20S; S8, C_{27} 5α,14α,17α(H)-cholestane 20R; S9, C_{28} 5α,14α,17α(H)-ergostane 20S; S10, C_{28} 5α,14β,17β(H)-ergostane 20R; S11, C_{28} 5α,14β,17β(H)-ergostane 20S; S12, C_{28} 5α,14α,17α(H)-ergostane 20R; S13, C_{29} 5α,14α,17α(H)-stigmastane 20S; S14, C_{29} 5α,14β,17β(H)-stigmastane 20R; S15, C_{29} 5α,14β,17β(H)-stigmastane 20S; S16, C_{29} 5α,14α,17α(H)-stigmastane 20R.

Table 2
Ratios (20) discussed in this study.

Sample	R1	R2	R3	R4	R5	R6	R7	R8	R9	R10	R11	R12	R13	R14	R15	R16	R17	R18	R19	R20
1	0.30	0.69	0.49	1.11	0.48	0.51	0.19	0.05	0.61	0.11	0.26	0.25	0.49	0.48	0.51	0.56	0.85	8.45	0.73	0.39
2	0.22	0.66	0.60	1.13	0.71	2.35	0.10	0.38	0.73	0.29	0.27	0.24	0.48	0.58	0.48	0.57	0.88	7.16	0.84	0.51
3	0.44	0.54	0.83	1.42	0.60	0.60	0.06	0.02	0.48	0.24	0.31	0.21	0.48	0.52	0.52	0.62	0.82	6.76	0.47	0.45
4	0.36	0.44	1.15	0.62	0.89	2.10	0.04	0.04	0.84	0.14	0.30	0.19	0.51	0.45	0.51	0.63	0.84	6.11	0.44	0.59
5	0.38	0.50	0.71	0.80	0.49	0.37	0.16	0.19	0.60	0.16	0.33	0.23	0.44	0.51	0.52	0.51	0.71	3.44	0.57	0.23
6	0.48	0.41	0.59	0.88	1.13	3.70	0.08	0.31	0.86	0.33	0.36	0.18	0.46	0.57	0.54	0.62	0.98	8.19	0.48	0.60
7	0.45	0.49	0.63	0.77	1.07	6.10	0.17	0.70	0.82	0.18	0.34	0.18	0.48	0.57	0.52	0.62	0.92	11.35	0.24	0.60
8	0.44	0.50	0.62	0.69	0.79	2.19	0.15	0.10	0.82	0.16	0.34	0.20	0.46	0.54	0.50	0.61	0.93	10.80	0.51	0.52
9	0.26	0.55	0.70	0.76	0.50	0.24	0.16	0.11	0.56	0.06	0.25	0.27	0.48	0.30	0.45	0.47	0.66	11.49	0.60	0.14
10	0.24	0.44	0.84	0.62	0.66	0.92	0.02	0.01	0.70	0.10	0.29	0.18	0.53	0.34	0.53	0.61	0.77	5.82	0.52	0.42
11	0.25	0.44	0.83	0.57	0.72	0.89	0.04	0.01	0.71	0.10	0.30	0.17	0.53	0.32	0.53	0.63	0.74	5.43	0.47	0.45
12	0.34	0.49	0.90	0.78	0.71	1.24	0.03	0.03	0.79	0.14	0.30	0.19	0.51	0.40	0.53	0.64	0.84	5.65	0.57	0.52
13	0.24	0.47	0.82	0.88	0.80	0.71	0.05	0.01	0.44	0.16	0.22	0.20	0.59	0.37	0.51	0.61	0.80	4.28	0.65	0.24
14	0.30	0.48	0.91	0.62	0.71	1.00	0.02	0.01	0.75	0.12	0.30	0.18	0.52	0.38	0.53	0.62	0.81	5.54	0.50	0.47
15	0.37	0.55	0.72	1.43	0.71	1.74	0.09	0.08	0.66	0.22	0.30	0.20	0.50	0.41	0.55	0.59	0.53	3.98	0.41	0.32
16	0.20	0.42	0.79	0.58	0.72	0.95	0.05	0.02	0.68	0.13	0.29	0.17	0.53	0.30	0.49	0.59	0.76	5.77	0.57	0.36
17	0.30	0.51	0.65	0.65	0.45	0.35	0.12	0.07	0.62	0.13	0.28	0.21	0.51	0.42	0.47	0.50	0.91	3.75	0.37	0.25
18	0.28	0.57	0.65	1.06	0.75	1.55	0.07	0.03	0.68	0.16	0.29	0.18	0.53	0.34	0.52	0.61	0.78	4.37	0.46	0.38
19	0.25	0.64	0.70	1.14	0.59	0.98	0.12	0.04	0.67	0.15	0.25	0.23	0.52	0.43	0.50	0.57	0.87	4.91	0.52	0.31
20	0.22	0.49	0.79	0.56	0.57	0.54	0.09	0.02	0.65	0.09	0.27	0.19	0.54	0.33	0.51	0.59	0.75	6.40	0.41	0.37
21	0.17	0.47	0.76	1.00	0.66	0.82	0.11	0.10	0.44	0.19	0.29	0.20	0.51	0.31	0.51	0.55	0.73	5.78	0.49	0.34
22	0.18	0.45	0.71	0.64	0.69	0.89	0.07	0.05	0.59	0.11	0.27	0.19	0.54	0.29	0.51	0.61	0.65	5.88	0.46	0.18
23	0.24	0.44	0.88	0.65	0.73	1.00	0.06	0.01	0.64	0.12	0.29	0.18	0.53	0.31	0.53	0.62	0.75	5.86	0.57	0.33
24	0.24	0.47	0.83	0.63	0.71	0.97	0.03	0.03	0.68	0.12	0.29	0.18	0.53	0.34	0.52	0.62	0.84	6.61	0.53	0.35
25	0.44	0.53	0.75	0.90	0.73	1.79	0.02	0.01	0.74	0.19	0.32	0.19	0.49	0.44	0.57	0.61	0.89	6.82	0.45	0.51
26	0.38	0.54	0.82	0.83	0.57	0.62	0.09	0.08	0.67	0.14	0.29	0.20	0.51	0.38	0.51	0.59	0.77	5.67	0.52	0.30
27	0.34	0.47	0.82	0.81	0.91	1.60	0.02	0.06	0.71	0.16	0.30	0.18	0.52	0.40	0.50	0.61	0.88	5.85	0.54	0.39
28	0.16	0.42	0.85	0.75	0.68	0.63	0.13	0.09	0.41	0.14	0.27	0.19	0.55	0.27	0.49	0.58	0.78	3.72	0.56	0.11
29	0.35	0.49	0.87	0.76	0.72	0.97	0.10	0.08	0.69	0.10	0.30	0.22	0.48	0.34	0.48	0.56	0.63	4.75	0.23	0.30
30	0.16	0.48	0.68	0.69	0.88	1.81	0.06	0.12	0.64	0.16	0.31	0.17	0.52	0.25	0.51	0.61	0.85	5.62	0.60	0.29
31	0.12	0.38	0.69	0.55	0.90	1.51	0.07	0.08	0.57	0.12	0.31	0.16	0.54	0.24	0.51	0.63	0.83	5.22	0.59	0.25
32	0.28	0.45	0.81	0.67	0.70	1.09	0.02	0.02	0.72	0.13	0.31	0.18	0.51	0.36	0.53	0.63	0.79	6.33	0.54	0.38
33	0.17	0.46	0.79	0.66	0.85	1.24	0.06	0.05	0.61	0.12	0.31	0.17	0.52	0.26	0.50	0.60	0.85	4.66	0.53	0.31
34	0.15	0.35	0.99	0.61	0.84	0.70	0.04	0.01	0.48	0.11	0.29	0.16	0.56	0.20	0.48	0.60	0.70	4.45	0.62	0.13
35	0.12	0.34	0.87	0.58	0.80	0.67	0.06	0.01	0.46	0.11	0.28	0.16	0.56	0.21	0.49	0.59	0.69	4.44	0.58	0.13
36	0.32	0.55	0.67	1.27	0.97	5.14	0.13	0.24	0.77	0.26	0.34	0.17	0.49	0.49	0.53	0.64	0.71	2.75	0.75	0.47
37	0.18	0.48	0.65	0.82	0.94	2.72	0.08	0.20	0.69	0.21	0.32	0.17	0.51	0.32	0.51	0.62	0.79	4.67	0.66	0.36
38	0.10	0.41	0.74	0.61	0.87	0.62	0.12	0.16	0.33	0.12	0.26	0.17	0.57	0.22	0.49	0.60	0.65	2.50	0.47	0.06
39	0.16	0.42	0.76	0.71	0.78	0.90	0.06	0.06	0.48	0.18	0.30	0.18	0.52	0.29	0.52	0.61	0.74	4.74	0.60	0.19
40	0.22	0.55	0.66	0.88	0.54	0.53	0.14	0.06	0.55	0.10	0.28	0.24	0.48	0.29	0.49	0.52	0.68	5.29	0.33	0.19
41	0.08	0.38	0.74	0.58	0.85	0.72	0.09	0.17	0.33	0.12	0.26	0.17	0.57	0.23	0.50	0.60	0.67	3.21	0.65	0.07
42	0.10	0.42	0.84	0.78	0.87	1.06	0.09	0.21	0.41	0.15	0.28	0.17	0.55	0.26	0.51	0.61	0.61	3.55	0.78	0.11
43	0.08	0.42	0.80	0.74	0.93	1.13	0.09	0.33	0.38	0.16	0.27	0.17	0.56	0.24	0.51	0.60	0.62	2.94	0.66	0.08
44	0.13	0.41	0.87	0.71	0.81	0.70	0.04	0.03	0.44	0.14	0.29	0.17	0.54	0.26	0.50	0.61	0.57	2.65	0.76	0.12
45	0.05	0.45	0.67	0.54	0.74	0.52	0.17	0.34	0.36	0.11	0.23	0.21	0.56	0.26	0.50	0.57	0.72	2.13	0.36	0.05
46	0.08	0.38	0.73	0.57	0.86	0.68	0.08	0.13	0.34	0.12	0.27	0.16	0.56	0.21	0.51	0.61	0.77	3.39	0.66	0.08
47	0.09	0.39	0.71	0.58	0.82	0.67	0.10	0.18	0.32	0.13	0.25	0.17	0.58	0.24	0.51	0.59	0.65	2.68	0.62	0.06
48	0.14	0.48	0.73	0.92	1.02	4.23	0.08	0.40	0.76	0.17	0.26	0.19	0.56	0.30	0.54	0.61	0.75	4.11	0.71	0.73
49	0.12	0.46	0.79	0.94	1.03	4.59	0.07	0.40	0.77	0.17	0.25	0.19	0.57	0.29	0.53	0.61	0.74	4.62	0.71	0.78
50	0.12	0.50	0.73	0.83	1.06	2.12	0.07	0.63	0.60	0.24	0.29	0.18	0.52	0.35	0.53	0.59	0.81	4.12	0.95	0.29
51	0.15	0.50	0.70	0.78	0.79	1.16	0.08	0.20	0.47	0.19	0.26	0.20	0.54	0.30	0.53	0.62	0.74	4.96	0.54	0.54
52	0.09	0.45	0.68	0.68	1.10	2.54	0.08	0.79	0.62	0.17	0.29	0.17	0.54	0.28	0.53	0.61	0.65	3.11	1.01	0.50
53	0.15	0.49	0.64	0.88	0.95	1.88	0.08	0.01	0.57	0.16	0.28	0.19	0.53	0.35	0.53	0.63	0.79	7.14	0.58	0.73
54	0.18	0.53	0.80	0.92	0.97	1.86	0.10	0.24	0.51	0.17	0.28	0.19	0.54	0.32	0.52	0.62	0.73	6.09	0.51	0.75
55	0.22	0.50	0.77	0.98	0.89	1.47	0.07	0.02	0.50	0.17	0.29	0.18	0.53	0.37	0.55	0.63	0.70	6.83	0.60	0.63
56	0.12	0.49	0.72	0.78	0.91	1.85	0.08	0.27	0.53	0.16	0.27	0.18	0.55	0.28	0.54	0.60	0.69	3.84	0.57	0.62
57	0.11	0.46	0.73	0.83	1.57	8.01	0.09	1.75	0.83	0.23	0.30	0.18	0.52	0.38	0.53	0.60	0.87	4.29	1.26	0.76
58	0.13	0.41	1.04	0.68	0.80	0.72	0.05	0.11	0.46	0.12	0.31	0.17	0.52	0.24	0.49	0.60	0.56	2.86	0.82	0.29
59	0.16	0.49	1.14	0.83	0.81	0.52	0.05	0.04	0.41	0.15	0.28	0.17	0.55	0.32	0.50	0.60	0.63	3.12	0.58	0.18
60	0.13	0.48	1.13	0.75	0.85	0.50	0.05	0.03	0.36	0.16	0.29	0.17	0.54	0.28	0.49	0.59	0.63	2.78	0.75	0.17
61	0.33	1.06	0.74	2.97	0.61	0.92	0.18	0.06	0.38	0.35	0.21	0.35	0.44	0.23	0.50	0.48	1.18	1.49	0.14	0.55
EM1	0.25	0.81	0.71	1.77	0.59	0.69	0.16	/	0.45	0.20	0.24	0.28	0.48	0.26	0.48	0.50	/	/	/	/
EM2	0.17	0.23	0.93	0.34	0.71	0.30	0.09	/	0.39	0.07	0.28	0.17	0.55	0.28	0.49	0.58	/	/	/	/
EM3	0.17	0.52	0.69	0.93	1.07	50.20	0.12	/	0.97	0.24	0.30	0.18	0.52	0.37	0.56	0.64	/	/	/	/

Note: The sample information is interpreted in the footnote to Table 1. R1 = C_{19}/C_{23}TT, [T1/T5]; R2 = C_{21}/C_{23}TT, [T3/T5]; R3 = C_{24}Te/C_{26}TT, [T8/T9]; R4 = C_{19-21}/C_{26-29}TT, [(T1 + T2 + T3)/(T9 + T10 + T11)]; R5 = $C_{29}H/C_{30}H$, [T14/T15]; R6 = $C_{23}TT/C_{30}H$, [T5/T15]; R7 = G/$C_{30}H$, [T18/T15]; R8 = 25-N$C_{29}H/C_{30}H$; R9 = Ts/(Ts + Tm), [T12/(T12 + T13)]; R10 = ∑preg/∑reg, [(S1 + S2)/(sum of S5 to S16)]; R11 = ∑C_{27}St/∑St, [(sum of S5 to S8)/(sum of S5 to S16)]; R12 = ∑C_{28}St/∑St, [(sum of S9 to S12)/(sum of S5 to S16)]; R13 = ∑C_{29}St/∑St, [(sum of S13 to S16)/(sum of S5 to S16)]; R14 = diaC_{27}/regC_{27} sterane, [(T3 + T4)/ (sum of S5 to S8)]; R15 = sterane C_{29}ααα20S/(20S + 20R), [S13/(S13 + S16)]; R16 = sterane C_{29}ββ/(αα + ββ), [(S14 + S15)/(sum of S13 to S16)]; R17 = MPI 1 = 1.5*(2-MP + 3-MP)/(P + 1-MP + 9-MP); R18 = MDR = 4-MDBT/1-MDBT; R19 = DBT/P; R20 = TAS(I)/TAS(I + II) = (C20 + C21 triaromatic pregnanes)/(C_{26}20S + C_{26}20R + C_{27}20S + C_{28}20S + C_{27}20R + C_{28}20R triaromatic steranes). The symbols for the biomarkers are described in footnote to Fig. 3.

Table 3
Concentrations (ppm, μg/g whole-oil) of steranes and whole-oil stable carbon isotope ratios for the oil samples.

Sample	S1	S2	S3	S4	S5	S6	S7	S8	S9	S10	S11	S12	S13	S14	S15	S16	$\delta^{13}C$, ‰
1	62	68	96	51	48	104	79	77	23	74	113	86	130	161	165	127	−31.96
2	251	107	126	70	43	127	84	83	30	72	108	89	124	170	167	134	−32.05
3	99	35	56	36	36	62	40	37	15	27	42	31	53	91	75	49	−32.19
4	67	28	60	35	24	81	59	46	20	33	48	28	67	110	111	64	−31.62
5	147	57	128	83	66	130	99	118	29	60	91	109	141	148	130	130	−31.37
6	117	33	55	38	33	57	33	40	23	12	28	19	43	64	64	36	−31.67
7	66	27	63	41	25	64	45	46	19	19	35	20	51	87	71	47	−31.65
8	53	21	48	33	26	54	33	39	18	18	29	24	40	65	60	40	−31.64
9	198	104	235	168	231	363	318	448	94	356	426	574	618	598	631	751	−31.47
10	110	58	104	60	69	184	144	82	28	79	118	66	179	268	251	156	−31.88
11	192	93	167	92	145	305	231	140	49	122	201	113	290	481	444	262	−31.93
12	101	47	79	50	48	125	87	64	28	48	83	49	105	166	186	92	−31.64
13	147	68	72	38	45	106	83	62	26	71	110	67	159	238	252	155	−32.28
14	136	63	118	76	92	189	142	87	39	79	130	68	181	285	275	157	−31.79
15	120	52	62	33	47	82	62	42	17	40	62	39	86	110	120	72	−31.31
16	228	89	130	81	120	262	209	124	39	107	175	97	259	407	362	273	−32.07
17	255	117	205	126	124	253	190	222	45	134	198	221	345	367	369	390	−31.41
18	176	84	100	60	68	178	134	85	28	79	118	73	174	263	254	157	−31.94
19	196	94	130	75	68	173	125	105	29	115	172	126	212	298	270	211	−31.73
20	157	82	133	88	98	246	201	135	30	124	190	144	282	384	418	270	−31.86
21	178	99	82	51	95	127	104	106	28	73	104	99	172	207	208	167	−32.79
22	202	102	132	84	105	273	222	138	36	143	196	137	291	467	421	274	−31.82
23	144	77	105	62	68	208	166	105	35	85	134	84	202	299	317	182	−31.97
24	124	65	95	60	62	173	130	89	31	68	107	69	159	253	253	148	−31.82
25	134	51	87	51	60	115	80	57	29	42	72	41	103	146	142	79	−31.60
26	151	62	109	67	97	155	119	92	24	81	123	86	169	245	228	160	−31.55
27	160	63	100	61	64	148	113	83	32	61	99	57	138	225	216	138	−31.60
28	266	130	134	81	156	266	204	164	39	139	201	165	333	450	471	346	−32.30
29	114	54	107	62	76	145	119	155	21	91	129	117	165	202	231	178	−31.51
30	291	135	126	82	153	295	228	158	42	118	185	109	274	450	406	265	−31.79
31	270	141	150	91	187	362	285	191	45	143	213	125	344	563	564	331	−31.92
32	139	68	116	66	83	180	145	98	37	77	113	63	165	259	265	148	−31.85
33	190	96	124	71	138	257	200	141	40	101	155	97	243	378	367	244	−31.72
34	193	106	96	58	154	263	218	149	26	122	169	109	291	452	460	321	−32.08
35	226	119	103	70	128	299	237	175	34	137	188	134	339	501	516	355	−32.15
36	122	44	66	40	37	79	55	44	20	25	43	21	61	100	100	53	−31.64
37	307	144	130	80	126	228	177	132	38	96	145	79	211	330	337	201	−31.79
38	84	46	41	24	43	107	84	58	17	53	69	55	125	199	188	130	−32.75
39	227	96	100	58	77	204	165	103	33	87	125	80	192	303	289	180	−32.42
40	225	124	178	96	160	286	237	257	120	177	226	271	372	425	410	389	−31.95
41	119	66	57	35	56	150	113	76	22	66	93	66	167	269	243	168	−32.95
42	271	152	125	77	148	274	215	140	48	118	182	114	299	472	448	287	−32.68
43	106	63	42	26	50	100	75	55	18	47	68	44	117	177	166	113	−32.80
44	411	195	202	121	231	434	341	231	70	191	283	179	449	713	678	442	−32.48
45	213	127	115	75	109	252	200	173	41	164	253	204	391	493	525	386	−32.85
46	294	156	133	85	186	361	282	192	47	168	232	156	424	659	623	402	−32.93
47	218	132	103	65	100	267	203	136	48	128	176	125	333	513	438	322	−33.16
48	425	233	186	108	156	362	283	179	84	171	285	165	440	679	610	377	−32.56
49	340	188	135	83	111	286	219	145	61	138	232	137	355	532	528	310	−32.55
50	302	136	116	73	69	209	149	110	52	80	125	77	206	310	255	185	−32.50
51	220	111	83	54	58	176	141	76	32	82	148	78	188	294	294	167	−32.40
52	340	191	157	105	166	328	252	175	73	136	203	128	353	557	506	317	−32.86
53	220	98	116	75	76	209	166	95	39	86	154	82	203	314	330	177	−32.41
54	273	152	137	80	122	252	206	107	43	109	211	101	264	443	383	244	−32.43
55	189	88	106	67	90	174	131	70	29	68	121	67	169	270	258	140	−32.65
56	187	123	91	54	72	197	160	95	37	85	152	87	232	337	318	200	−32.28
57	423	191	181	119	150	279	185	180	82	119	161	118	287	436	385	257	−32.98
58	217	138	136	79	166	323	261	160	41	141	192	129	303	482	446	309	−32.81
59	176	113	114	61	83	204	151	110	37	85	115	88	216	346	296	219	−33.50
60	199	129	110	60	83	227	174	119	34	92	120	93	223	342	320	229	−33.76
61	632	329	85	52	126	151	144	167	151	233	279	295	317	294	282	319	−28.80
EM1	683	359	194	123	233	345	301	343	177	348	434	477	590	619	606	627	−29.42
EM2	76	44	84	51	76	168	132	102	15	78	109	89	188	273	271	199	−32.57
EM3	363	168	154	94	113	253	186	113	62	93	169	69	231	388	353	179	−31.74

Note: The sample information is interpreted in the footnote to Table 1. The symbols of the biomarkers (S1–S16) are described in footnote to Fig. 3. The EM1, EM2 and EM3 oils are the endmembers and their biomarker concentrations are calculated by ALS-C. The calculation method is described in Section 3.3.2. The related data are shown in the Appendix.

Uplift as well as the C_{30}–C_{34}-norhomohopane series, C_{26}-nortrinorhopanes, 17-nortricyclic terpanes in some oils (Fig. 6), indicating these oils have been biodegraded. The UCM in GC is one line of evidence for biodegradation. *n*-Alkanes are the first compound class consumed during biodegradation. Severely biodegraded oils generally lack alkane peaks but display various sizes of the UCM. Almost all oil samples from the Tarim Basin display biodegradation signatures, including variable UCM and significant

Table 4
Concentrations (ppm) of terpanes used in the biomarker concentration dataset.

Sample	T1	T2	T3	T4	T5	T6	T7	T8	T9	T10	T11	T12	T13	T14	T15	T16	T17	T18	T19	T20	T21	T22	T23	T24
1	97	275	224	50	326	203	161	83	172	196	168	134	87	303	637	318	172	122	199	139	169	92	69	55
2	134	441	408	111	619	393	311	177	296	269	307	204	76	188	264	85	64	27	47	32	58	29	31	41
3	83	168	102	31	189	105	80	67	80	81	86	89	95	189	314	116	87	18	102	71	46	49	39	29
4	65	88	80	23	181	117	98	100	88	110	176	152	29	76	86	71	39	3	29	45	41	30	28	22
5	113	178	150	46	301	194	157	114	162	174	216	205	135	391	803	209	152	125	144	128	127	88	51	51
6	63	106	54	24	133	85	73	40	68	91	96	60	10	40	36	28	35	3	27	40	0	0	0	0
7	64	103	69	22	142	105	92	56	88	107	110	76	17	25	23	37	75	4	59	50	36	35	30	19
8	43	66	50	13	99	72	68	43	70	71	89	69	15	36	45	52	61	7	50	47	38	33	0	0
9	137	318	289	80	525	323	270	212	301	326	346	426	334	1082	2171	732	454	356	425	309	360	207	163	137
10	95	196	176	60	397	273	246	163	194	238	318	217	95	284	432	199	140	11	156	109	103	77	70	45
11	156	283	275	96	621	451	381	267	323	412	509	350	145	502	700	299	229	27	260	195	187	96	126	86
12	96	167	142	42	287	209	159	134	149	168	203	189	51	165	231	65	75	7	75	55	45	50	32	45
13	99	200	192	72	406	248	223	156	190	174	191	178	229	459	572	272	198	27	195	153	143	101	79	78
14	128	207	205	65	428	299	259	207	228	297	344	282	91	302	427	203	131	7	157	111	85	74	68	45
15	144	240	215	73	391	236	182	105	145	125	150	104	54	159	224	98	68	21	63	48	41	33	29	16
16	124	248	258	93	619	433	359	245	312	338	441	307	145	472	654	291	221	30	243	175	187	101	118	73
17	171	277	288	99	567	408	312	246	379	363	399	434	268	724	1610	421	294	189	300	257	253	140	107	79
18	158	336	324	96	570	393	292	161	246	235	288	186	90	276	367	143	133	27	129	97	126	44	57	43
19	146	397	373	107	579	343	262	179	257	252	295	241	120	351	594	285	157	70	153	110	185	77	72	41
20	107	216	245	76	498	343	307	219	276	349	384	320	171	519	918	307	232	85	248	211	244	115	147	117
21	88	252	244	98	520	288	242	160	210	174	201	179	229	418	636	254	190	72	175	129	119	70	68	52
22	134	339	336	123	742	514	431	245	347	406	509	279	197	574	833	486	229	60	266	208	221	85	106	74
23	119	224	220	78	503	349	284	191	217	288	358	227	130	365	501	269	171	29	201	152	132	73	77	63
24	94	188	182	59	385	273	230	159	191	248	292	197	94	283	399	166	131	12	153	114	111	57	55	51
25	145	199	175	43	333	243	185	124	166	185	226	146	51	136	186	109	72	3	79	60	0	0	0	0
26	143	226	202	57	371	261	226	159	194	215	278	212	106	340	599	197	147	51	154	110	114	69	79	48
27	139	236	192	65	411	297	255	171	208	226	264	192	77	235	257	112	79	5	92	79	66	50	32	25
28	125	333	329	142	781	462	399	272	319	346	385	263	374	841	1239	616	408	161	418	332	341	165	175	142
29	109	182	150	48	308	213	185	145	167	194	219	206	94	229	317	128	103	31	97	65	72	45	37	25
30	134	495	413	136	865	653	516	274	405	462	644	243	137	422	479	247	178	29	183	147	176	100	85	66
31	136	463	423	165	1112	795	663	349	503	568	801	292	223	664	735	349	274	54	313	230	204	134	121	84
32	120	220	189	73	425	310	248	178	219	271	304	226	88	273	391	182	131	9	144	112	103	70	70	49
33	127	325	332	118	724	511	418	253	322	396	477	246	161	495	582	286	188	35	214	153	147	87	88	53
34	121	277	292	129	827	497	418	299	302	369	467	310	341	982	1176	734	464	46	508	374	420	208	206	147
35	115	308	316	143	930	545	459	331	378	381	520	337	389	1117	1396	834	532	77	552	429	472	248	242	168
36	103	230	175	56	319	222	167	89	133	120	147	84	25	60	62	59	30	8	27	19	25	27	0	0
37	136	527	373	123	773	590	440	233	361	396	505	197	88	268	284	127	112	24	110	85	98	65	98	49
38	32	103	132	51	325	184	176	100	135	138	165	98	200	451	520	286	204	63	206	157	152	87	84	59
39	90	243	232	99	552	353	286	179	236	261	300	190	202	479	612	353	209	39	220	174	159	88	104	60
40	181	393	457	154	832	528	426	244	372	389	414	336	275	860	1580	532	327	225	349	256	275	182	143	0
41	35	135	178	82	463	256	231	134	181	193	222	126	255	553	647	362	237	56	264	194	182	105	101	70
42	109	394	445	188	1066	606	510	322	383	387	448	277	396	870	1001	547	387	92	390	294	337	170	164	128
43	32	130	167	71	401	225	192	120	150	133	165	103	168	331	356	193	136	34	140	110	111	60	64	46
44	184	549	572	248	1385	891	736	502	575	541	723	462	595	1615	1984	1063	676	81	756	549	593	300	330	219
45	42	220	358	144	801	453	443	260	389	356	394	304	551	1141	1545	648	459	269	454	339	364	217	211	135
46	90	329	410	181	1074	609	554	324	442	461	558	299	590	1360	1573	912	625	125	690	511	471	265	267	211
47	79	256	348	157	892	494	475	257	363	371	444	236	504	1085	1328	702	485	127	522	400	364	218	241	189
48	206	731	717	285	1508	965	793	469	641	475	678	415	128	363	356	177	146	29	128	110	94	94	58	58
49	151	608	583	244	1263	794	646	382	482	406	535	336	102	285	275	139	125	18	95	83	76	51	97	67
50	114	415	471	193	952	541	465	288	394	351	462	241	162	478	449	228	177	31	178	128	119	86	75	64
51	96	316	330	121	660	442	346	205	292	274	384	175	198	452	569	240	174	45	154	124	128	87	69	52
52	124	507	621	266	1375	812	704	394	576	546	728	321	199	595	541	301	243	44	195	144	175	101	84	81
53	99	332	319	114	645	410	331	167	260	264	331	165	126	327	342	176	131	28	123	96	77	57	47	33
54	135	449	399	132	748	508	377	262	327	312	432	196	189	388	402	178	127	40	129	100	111	81	0	0
55	118	313	273	94	542	343	262	169	220	228	268	155	153	327	368	179	139	27	134	96	91	39	0	0

(*continued on next page*)

Table 4 (*continued*)

Sample	T1	T2	T3	T4	T5	T6	T7	T8	T9	T10	T11	T12	T13	T14	T15	T16	T17	T18	T19	T20	T21	T22	T23	T24
56	83	324	339	130	686	460	364	216	302	280	376	163	148	337	371	155	128	28	110	93	69	63	52	36
57	174	676	722	319	1586	879	731	450	620	555	717	354	75	310	198	148	127	19	78	70	173	86	0	0
58	115	337	356	145	860	526	443	350	336	378	480	332	391	959	1197	717	467	58	463	336	341	162	159	133
59	70	206	209	81	427	265	220	195	171	189	228	188	271	669	828	457	320	40	339	264	211	145	123	89
60	68	241	247	94	510	316	264	240	212	252	279	218	395	874	1028	582	414	48	396	308	256	153	155	109
61	360	1386	1154	213	1093	500	377	250	339	439	199	273	444	720	1190	330	231	213	167	123	83	69	54	35
EM1	373	1375	1226	289	1520	795	630	406	570	625	487	483	597	1287	2195	721	469	351	419	313	322	194	163	100
EM2	50	66	66	39	287	182	171	134	144	177	211	181	281	688	964	492	326	82	353	268	259	143	145	106
EM3	199	663	607	220	1169	776	608	340	496	458	621	277	10	25	23	28	30	3	27	19	0	0	0	0

Note: The sample information is interpreted in the footnote to Table 1. The symbols of the biomarkers (T1–T24) are described in footnote to Fig. 3.

amounts of 25-norhopanes and 17-nortricyclic terpanes (Zhang et al., 2014). Despite these indications of biodegradation, the investigated oils from the Tabei Uplift show complete *n*-alkanes and isoprenoids series. The co-existence of 25-norhopanes, intact *n*-alkanes and clear UCM indicate that the studied oils are mixtures of biodegraded oil with later charge by non-biodegraded oil. Multiple-stage oils may be generated from the same source rock at different maturities and/or from diverse source rocks having the same or different maturities.

4.2.2. Maturity parameters

Some parameters based on the stability or transformation of molecules have been established to assess oil maturity. Because of the differences of reaction endpoints and response, the maturity parameters have different application scope. For the oil samples in our study, commonly used aliphatic biomarker maturity parameters show different maturity ranges relative to the oil window. For example, the values of C_{29} steranes 20S/(20S + 20R) and ββ/(ββ + αα) are typically less than or equal to their equilibrium endpoints, indicating oils generated in the early to peak oil window stage (Fig. 5a). Ratios of $diaC_{27}/regC_{27}$ and Ts/(Ts + Tm) change over a large range for the samples (Table 2) and show a positive correlation (Fig. 5b), indicating oils generated throughout the oil window. For biodegraded oils and high maturity oils, aromatic hydrocarbon ratios can potentially be more useful, as they are resistant to biodegradation and sensitive to maturity differences in the middle to late parts of the oil window. In our samples, we found a good positive correlation between MPI1 and MDR (Fig. 5c). The equivalent vitrinite reflectance values %Rc1 and %Rc2 for the oils range from 0.72 to 0.99 and 1.10 to 1.55, calculated by the equations of %Rc1 = 0.6 × MPI1 + 0.4 (Radke and Welte, 1983) and %Rc2 = 0.2633 × ln(MDR) + 0.9034 (Dzou et al., 1995), respectively. The %Rc2 in this study is similar to %Rc3 (0.90–1.74) calculated from the methyl diamantane index (MDI, Zhang et al., 2005), using %Rc3 = 2.4389 × MDI + 0.4364. The value of MDR or %Rc2 indicates the oils were generated at moderately high maturity. Relatively low%Rc1 values may be due to a reversal of MPI1 at high maturity levels (>1.35%, Radke and Welte, 1983). The inconsistency between aliphatic and aromatic maturity parameters and the positive correlation between diverse maturity parameters in the oil samples may indicate that the oils are mixtures of hydrocarbons from more than one source or more than one generation episode from the same source (Zhang et al., 2005).

4.2.3. Carbon isotope ratios of whole oil and fractions

The relationship between stable carbon isotope ratios of whole oil and fractions was discussed by Peters et al. (2005). Petroleum shows increased ^{13}C for fractions of increasing polarity and boiling point. Because the fractions are generated during thermal cracking of kerogen, kinetic fractionation is expected to enrich the kerogen in ^{13}C, while the fractions become relatively depleted in the order of decreasing polarity: asphaltenes > NSO-compounds > aromatics > saturates. Whole oil or bitumen generally has an isotopic composition between the saturated and aromatic hydrocarbons because these account for the bulk of most petroleum samples.

However, the carbon isotope ratios of oil fractions from the Tabei Uplift have inconsistent isotopic patterns. There is little difference in ^{13}C content between fractions for studied oil samples and in some oils, complete or partial reversals have been found (Fig. 7), *i.e.*, ^{13}C becomes relatively depleted in the order: saturates > whole oil > aromatics > NSO-compounds > asphaltenes or saturates > whole oil or aromatics > NSO-compounds > asphaltenes. Although special organic matter contributions cannot be excluded, this can also be explained by oil mixing (Wang et al., 2004). For the same source rock, oils generated at an earlier stage have lower maturity and are enriched in polar fractions and

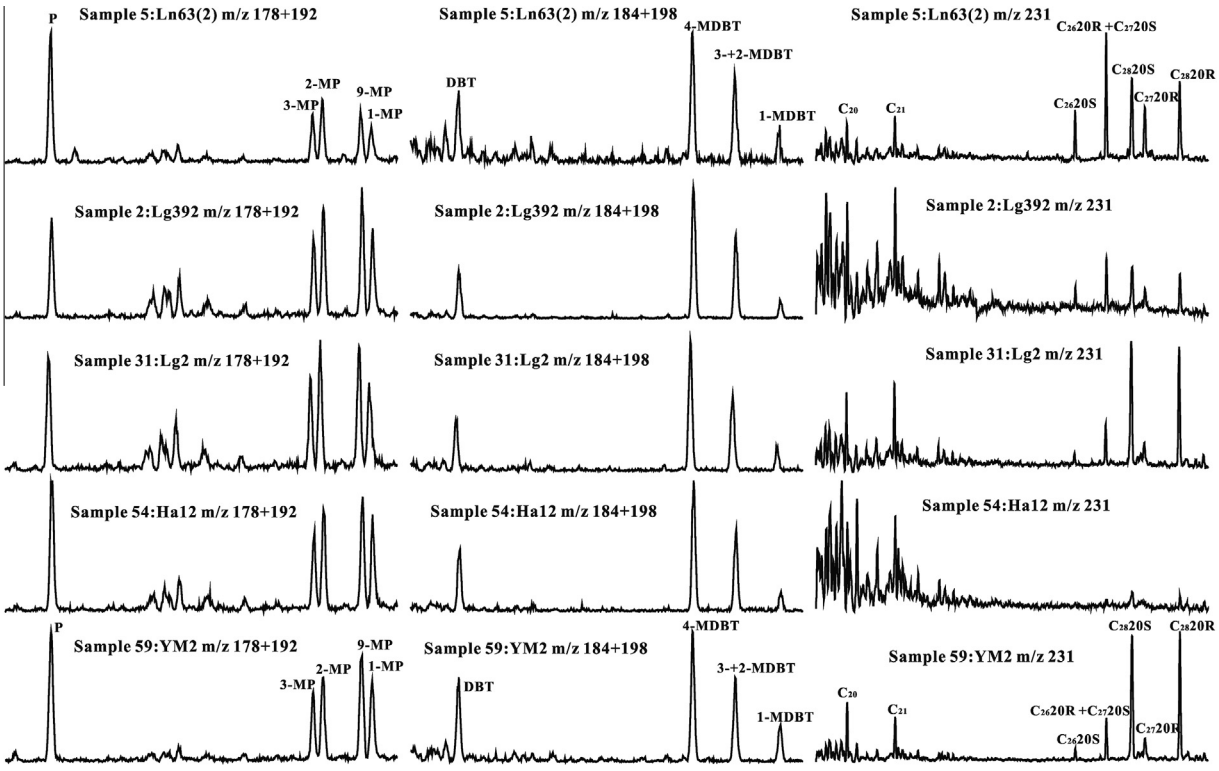

Fig. 4. Representative *m/z* 178 + 192, 184 + 198 and 231 mass fragmentograms showing the distribution of phenanthrene, dibenzothiophene series and triaromatic steroids, respectively. *Note:* P, phenanthrene; MP, methylphenanthrene; DBT, dibenzothiophene; MDBT, methyldibenzothiophene; C_{20-21}, C_{20-21} triaromatic preganes.

depleted ^{13}C than those generated at later stage. If early oil was severely biodegraded in the reservoir, leaving asphaltenes and NSO-compounds, then heavy oil with relatively depleted ^{13}C for polar fractions will be formed. When late fresh oil mixed with early biodegraded oil in the reservoir, the mixture could exhibit carbon isotope features similar to what we see in our oils from the Tabei Uplift. Although these differences in ^{13}C between oils or fractions ^{13}C are no more than 2–3‰, this mixing process can account for complete or partial ^{13}C reversals between fractions of the Tabei Uplift oil samples.

4.2.4. Scores of PCA

Principal component analysis (PCA), another kind of multivariate statistical method, concentrates relevant information from complex *n*-dimensional data into a few dimensions. The objective of PCA is to reduce the dimensionality of source-related geochemical data to a few components that best explain the variation in the data (Peters et al., 2005). For PCA, a plot of PC1 versus PC2, also called a scores plot, represents the best two-dimensional separation of the samples into genetic groups from *n*-dimensional space. PCA was used to distinguish 61 oil samples from the Mahakam Delta area of Kalimantan, Indonesia, as exemplified by a principal component scores plot of PC1 and PC2 (Peters et al., 2005). In our previous study, 64 laboratory samples created by mixing of three different endmember oils were differentiated using a triangular scores plot of PCA based on the concentrations of 43 biomarkers and whole-oil stable carbon isotope ratios (Zhan et al., 2016).

In our present study, 61 oil samples (60 from the Tabei Uplift and one from the Tazhong Uplift) were analyzed by PCA based on the concentrations of 40 biomarkers and whole-oil stable carbon isotope ratios (Tables 2 and 3). They are scattered as an approximately triangular distribution on both the three-dimensional scores plot (PC1 vs. PC2 vs. PC3, Fig. 8a) and the two-dimensional scores plot (PC1 vs. PC2, Fig. 8b). This suggests that the samples are mixed oils.

4.3. De-convoluting mixtures

4.3.1. Unmixing the mixed oils

The number of endmembers (maximum sources in ALS) for the mixed oil samples from the Tabei Uplift was identified as three based on ALS and geological considerations. The cumulative variance accounted for by three sources was 96.0%, meeting the requirements of multivariate statistical analysis (*i.e.* generally not less than 90%). This conclusion is also supported by previous studies which verified the oils in the Palaeozoic reservoirs of the Tarim Basin originated from the Cambrian–Lower Ordovician and Middle–Upper Ordovician marine source rocks having different maturities (Li et al., 2010, 2015; Yu et al., 2011; Zhu et al., 2012, 2013, 2014b; Tian et al., 2012b; Tian, 2013).

Biomarker concentrations are more suitable than ratios for ALS to de-convolute mixed oil (Peters et al., 2008b; Zhan et al., 2016). In this study, the relative contributions and compound compositions of the endmember oils (EM1, EM2, EM3) were calculated by ALS-C using a normalized dataset of 40 biomarker concentrations and the whole oil carbon isotope ratios. The values of the relative contributions of EM1, EM2 and EM3 for the oils in the Tabei Uplift are shown in Table 6. EM1 corresponds to Tz62 Silurian oil and it is the minimum contributor for the mixtures. EM2 is the secondary contributor. EM3 is the major contributor for most oils and its proportions range from 13% to 95%. The biomarker molecular compositions of the three endmember oils are shown in Tables 3 and 4. Some biomarker ratios of endmember oils were obtained using related compound concentrations computed by ALS-C and shown in Table 2.

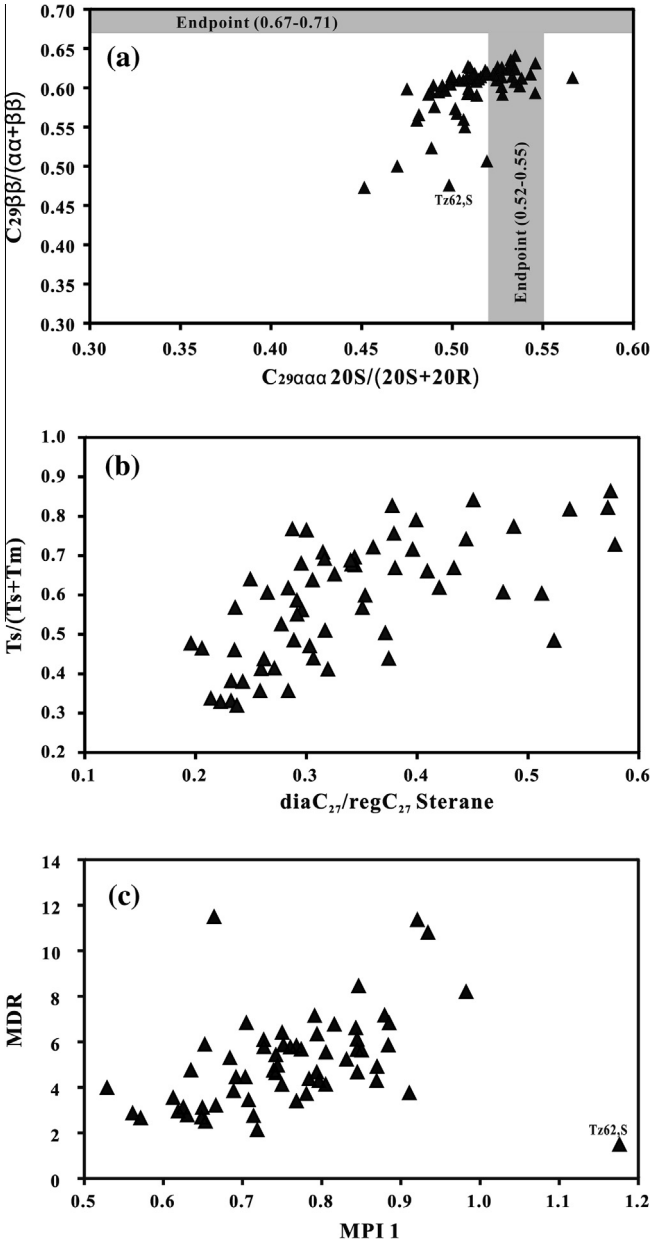

Fig. 5. Correlations of ratios of (a) C_{29} sterane 20S/(20S + 20R) vs. ββ/(ββ + αα), (R15 vs. R16) (b) Ts/(Ts + Tm) vs. $diaC_{27}/regC_{27}$ sterane, (R9 vs. R14) and (c) MDR vs. MPI 1, (R18 vs. R17) in the oil samples from the Tabei Uplift. Compound symbols are described in the footnotes of Figs. 3 and 4. Ratio symbols and values are described in the footnotes of Table 2.

4.3.2. Geological significance of the endmember oils

There are some similarities and differences in the three endmember oils, depending on parameters related to source or depositional setting. The EM2 and EM3 oils have similar sources and differ from the EM1 oil. The carbon isotopic ratios ($\delta^{13}C$) are −29.42‰, −32.57‰ and −31.74‰ for the EM1, EM2 and EM3 oils (Table 2), respectively. The normalized relative abundances of C_{28} steranes ($\sum C_{28}$) in C_{27}–C_{29} regular steranes are 0.28, 0.17 and 0.18 for the EM1, EM2 and EM3 oils (Table 5), respectively. The C_{28}/C_{29} sterane ratio has source- and age- significance (Peters et al., 2005), and is 0.59, 0.31 and 0.34 for the three endmember oils (Table 2), respectively. The $G/C_{30}H$ ratio is a specific parameter for water-column stratification (commonly resulting from hypersalinity) during source-rock deposition (Peters et al., 2005) and is 0.16, 0.09 and 0.11 for the EM1, EM2, and EM3, respectively (Table 2). These parameters are relatively resistant to alteration by maturation and biodegradation and indicate that the EM1 oil originated from an older source rock deposited in a more saline setting than that for the EM2 and EM3 oils.

According to biomarker maturity parameters, the EM1 and EM2 oils are less mature than the EM3 oils. For example, the C_{29} sterane 20S/(20S + 20R) and ββ/(ββ + αα) ratios are 0.48 and 0.50 for EM1, 0.49 and 0.58 for EM2, all being before the equilibrium endpoints, and 0.56 and 0.65 for EM3, approaching the endpoint (Table 2), respectively. The ratios of Ts/(Ts + Tm) and $diaC_{27}/regC_{27}$ are 0.45 and 0.26, 0.39 and 0.28, 0.97 and 0.37 for EM1, EM2 and EM3 (Table 2), respectively. These show that the EM3 oil has higher maturity and is in the late oil generation stage; while the EM1 and EM2 oils have relatively low maturities and are in the early to peak oil generation stage. Similar conclusions can be deduced based on the concentrations of maturity-resistant biomarkers even though the oils are affected by other processes, such as biodegradation. For example, the EM2 and EM3 oils have the same source and different biomarker concentrations. The EM3 oil has only a small amount or no hopanes and has relatively high concentrations of tricyclic terpanes and steranes, which is the opposite of the EM2 oil. This is attributable to the fact that tricyclic terpanes and steranes have higher thermal stabilities than hopanes. In addition, we conclude that biodegradation also enriched biomarkers in the EM2 and EM1 oils. Since tricyclic terpanes are more resistant to biodegradation than the hopanes this can also explain differences in some parameters based on tricyclic and pentacyclic terpanes between the EM2 and EM3 oils.

There are a few studies of marine source rocks from the Cambrian–Lower Ordovician and the Middle–Upper Ordovician. Source-related biomarker ratios for extracts from previous studies in the Tarim Basin are shown in Table 5 (Cai et al., 2009b; Chang et al., 2013; Guo et al., 2008; Li et al., 2012; Zhang et al., 2000, 2004; Zhu et al., 2014a). Based on the correlation of the source-related biomarker ratios from endmember oils and source rocks, it can be concluded that EM1 oil originated from Cambrian–Lower Ordovician source rocks, while the EM2 and EM3 oils originated from Middle–Upper Ordovician source rocks at different stages of maturity; the maturity of the EM2 oil being lower than EM3.

The biomarker compositions (concentrations) of endmember oils from ALS-C cannot directly be used to interpret the geological and/or geochemical processes. However, ratios or distributions of biomarkers can be used to correlate oils with extracts of source rocks to ascertain the origin of the endmember oils. The geological significance of endmember oils from ALS-C must be deduced based on petroleum geology and must indicate a coherent set of processes such as hydrocarbon charging, accumulation, and mixing.

There is no sample in the investigated oils from the Tabei Uplift that is completely in accordance with the endmember oil from ALS-C. The Tz62 Silurian oil (from the Tazhong Uplift) approaches the endmember composition and is believed to represent of endmember oils derived from Cambrian–Lower Ordovician source rocks. However, the Tz62 Silurian oil is identified as a mixture based on the co-existence of 25-norhopanes, intact *n*-alkanes and a pronounced UCM (Xiao et al., 2005). Jia et al. (2013) also doubted that the Tz62 Silurian oil is an endmember oil based on hydrogen and carbon isotopic compositions of *n*-alkanes and whole oil. Furthermore, the maturity parameters for this sample show inconsistencies between the aliphatic and aromatic parametersfractions. The C_{29} sterane 20S/(20S + 20R) and ββ/(ββ + αα) ratios (0.48 and 0.50, respectively) indicate relatively low maturity; while the value of MPI1 (1.18) reached an equivalent vitrinite reflectance 1.11% or 1.59%, indicating relatively high maturity. The early low maturity oil was probably biodegraded oil derived from Cambrian–Lower Ordovician source rocks or severely biodegraded remnants of that

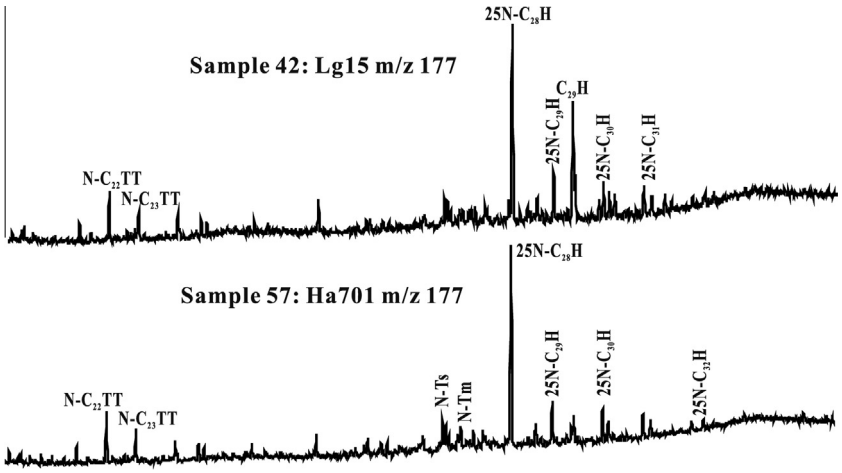

Fig. 6. Representative *m/z* 177 mass fragmentograms showing 17-nortricyclic terpane (N-TT) and 25-norhopane (N-H) distributions.

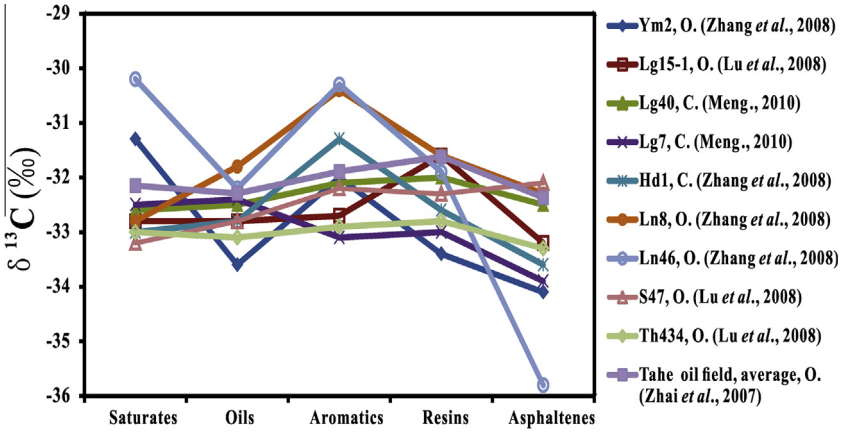

Fig. 7. Carbon isotope ratios ($\delta^{13}C$, ‰) of whole oil and fractions of the oils from the Tabei Uplift. Complete or partial reversals in the $\delta^{13}C$ of fractions may indicate geological mixing of oils generated from different source rocks with diverse $\delta^{13}C$ or from the same rocks at different maturities. The data for this figure are in Appendix 3. (See above-mentioned references for further information.)

oil extracted by late high maturity oil during migration. Therefore, the EM1 oil from ALS-C represents early biodegraded oil in the Tabei Uplift derived from Cambrian–Lower Ordovician source rocks. This conclusion can also be proven by the biomarker concentrations of EM1, which are generally greater than the corresponding compounds in Tz62 Silurian oil.

4.4. Multiple charging and mixing model

Many publications document the tectonic evolution of the Tabei Uplift and petroleum generation and expulsion from the two main marine source rocks. Previous research (Li et al., 2010, 2015; Yu et al., 2011; Zhu et al., 2012, 2013, 2014b and references therein) and the de-convolution results for mixed oils in our study indicate that three stages of petroleum charge and two phases of biodegradation and mixing occurred in Palaeozoic reservoirs of the Tabei Uplift.

The first charge occurred during the late Caledonian orogeny. Abundant petroleum from Cambrian–Lower Ordovician source rocks charged Palaeozoic reservoirs in the Tabei Uplift. However, because of uplift during the early Hercynian, the oils were severely biodegraded and only residual heavy oil remained in local areas. This charge may represent the bulk of the widely distributed Silurian bitumen sand and solid bitumen. The second charge and first mixing event took place during the late Hercynian orogeny. At the end of the Permian period, large amounts of petroleum generated from Middle–Upper Ordovician source rocks in the early oil generation stage, as well as some oil from the upper part of the Cambrian–Lower Ordovician source rock, migrated along faults and unconformities into the Palaeozoic reservoirs and mixed with the residual oils of the first charge. Subsequent uplift exposed the mixtures to biodegradation, resulting in heavy oil dominated by asphaltenes and NSO-compounds with relatively depleted ^{13}C. The third charge and second mixing event took place probably during the late Yanshan to Himalayan orogeny from the end of the Cretaceous to the Neogene. This was the most important stage of petroleum accumulation for the Palaeozoic reservoirs in the Tabei Uplift. The third oil charge likely originated from Middle–Upper Ordovician source rocks in the late oil generation stage and combined with the previous residual mixtures. The final mixtures were not biodegraded further, but other secondary processes (such as evaporative fractionation or gas washing) cannot be excluded, and can result in different distributions of alkanes. Crude oil mixtures from this final phase are now being produced from the Palaeozoic reservoirs in the Tabei Uplift.

In the final mixtures, the remnant of the first stage charge, derived from the Cambrian–Lower Ordovician source rock in the early to peak oil generation stage, corresponds to EM1, which is the minimum contributor to the Tabei Uplift Palaeozoic marine oils, accounting for less than 10% of most oils. This oil is the residue

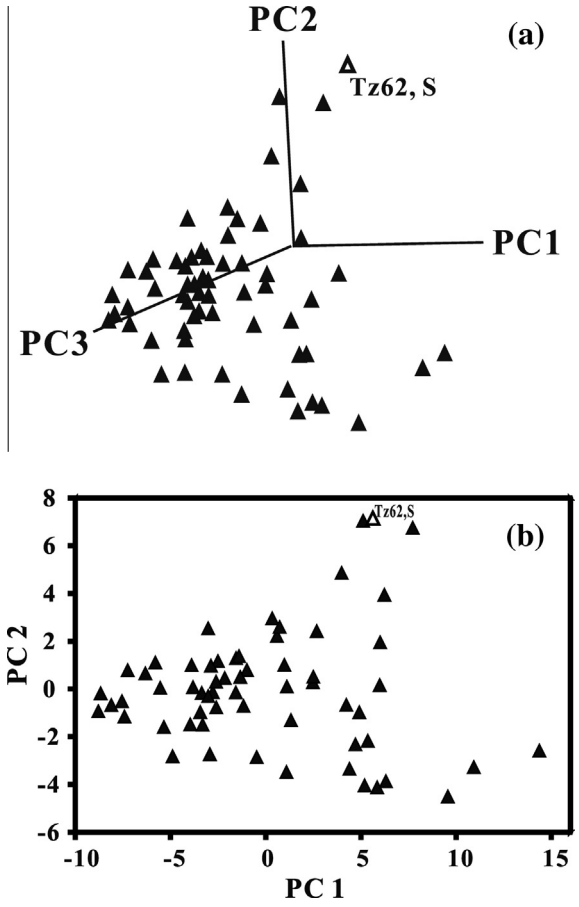

Fig. 8. The three-dimensional scores plot (a) and two-dimensional scores plot (b) by PCA based on the concentration dataset and the whole-oil stable carbon isotopic ratios (Tables 2 and 3). The samples scattered as an approximately triangular distribution on both of them, indicating that they are mixtures. PC1, PC2 and PC3 are principal components accounting for 65.0%, 15.9% and 8.0% of the variance in the data, respectively.

of two phases of biodegradation and has the highest concentration of biomarkers. The remnant of the second stage charge in the final mixtures, mainly derived from the Middle–Upper Ordovician source rocks in the early oil generation stage, corresponds to EM2, which is the secondary contributor, and its proportions are in the range of 10–40% in most oils. This oil is the residue of one phase of biodegradation and has relatively high concentrations of biomarkers. The third charge of oil in the final mixtures corresponds to EM3, which is the major contributor to most oils with proportions in the range of 13–95% and on average of 64%. This oil has high maturity and low concentrations of biomarkers. The intact *n*-alkanes and part of the aromatics fraction in all oils come from this oil charge. As a result, the *n*-alkanes and total oils in the Tabei Uplift have similar hydrogen and carbon isotopic compositions (Jia et al., 2013; Li et al., 2010, 2015) and aromatic maturity parameters that are high. The biomarkers in the final mixtures mainly reveal mixed characteristics of the former two charge oils and low relative thermal maturity.

This model does not include any information about petroleum generated from the Cambrian–Lower Ordovician source rocks in the late oil generation stage. There are three possible reasons: (i) these oils were generated and expelled from the source rocks before the late Hercynian orogeny, but did not accumulate because of ineffective migration pathways, reservoirs, or cap rocks. (ii) These high maturity oils had low concentrations of biomarkers, asphaltenes and NSO-compounds. They charged the same reservoirs and mixed with remnants of the first charge, but they were severely biodegraded without leaving significant amounts biomarkers and thus have no response on ALS-C. (iii) These oils accumulated in Palaeozoic or shallower reservoirs as light oil and condensate. These kinds of oil have not been recovered or the samples were excluded from the study due to very low biomarkers. More samples and further research are needed to determine whether this oil type exists.

5. Conclusions

Palaeozoic reservoirs are the most significant exploration target in the Tabei Uplift of the Tarim Basin. They contain petroleum ranging from heavy oil, light oil, condensate, wet gas and dry gas. Crude oils recovered from the Ordovician and Carboniferous reservoirs are mixtures of oil having different maturity from diverse source rocks based on: (i) co-existence of 25-norhopanes, intact *n*-alkanes and prominent unresolved complex mixtures (UCM); (ii) inconsistent biomarker and aromatic maturity parameters; (iii) reversals of $\delta^{13}C$ between fractions of oil; and (iv) score plots of principal component analysis (PCA). Three endmember oils, EM1, EM2 and EM3 were identified by alternating least squares regression using a normalized dataset of 40 biomarker concentrations and whole-oil carbon isotope ratios (ALS-C). The EM2 and EM3 oils were generated from Middle–Upper Ordovician source rocks, but the maturity of EM2 is less than EM3. EM1 oil was

Table 5
Source-related biomarker parameters and $\delta^{13}C$ of the extracts from marine source rocks of the Tarim Basin summarized from references.

Well	Formation	^{13}C of extracts or end member	$C_{29}H/C_{30}H$	$G/C_{30}H$	$\sum C_{27}$	$\sum C_{28}$	$\sum C_{29}$	References
TZ12	O_3	/	0.66	0.05	0.32	0.24	0.44	Cai et al. (2009b), Li et al. (2012)
LN46	O_{2-3}	−31.8	0.84	0.11	0.26	0.19	0.55	Cai et al. (2009b), Chang et al. (2013), Li et al. (2012)
He3	O_3	/	0.57	0.07	0.31	0.22	0.47	Cai et al. (2009b)
Z11	O_3	/	0.54	0.06	0.23	0.17	0.60	Cai et al. (2009b)
TZ30	O_{2-3}	−31.7	0.58	0.09	0.33	0.20	0.47	Li et al. (2012), Chang et al. (2013)
TD2	Cam.	−28.6	0.49	0.18	0.31	0.27	0.39	Cai et al. (2009b), Chang et al. (2013), Li et al. (2012)
KN1	Cam.	−29.1	0.48	0.15	0.28	0.30	0.41	Cai et al. (2009b), Chang et al. (2013), Li et al. (2012)
H4	Cam.	−26.1	0.36	0.20	0.10	0.35	0.55	Chang et al. (2013)
H3	Cam.	−26.1	0.57	0.10	0.22	0.35	0.43	Chang et al. (2013)
YL1	Cam.-O_1	/	0.52	/	0.34	0.26	0.41	Guo et al. (2008), Li et al. (2012)
XH1	Cam.	−28.61	0.52	/	0.28	0.35	0.37	Zhu et al. (2014a)
EM1		−29.4	0.59	0.16	0.24	0.28	0.48	Calculated by ALS-C
EM2		−32.6	0.71	0.09	0.28	0.17	0.55	Calculated by ALS-C
EM3		−31.7	1.07	0.12	0.30	0.18	0.52	Calculated by ALS-C

Note: O_3, upper Ordovician; O_{2-3}, Middle–Upper Ordovician; Cam., Cambrian; O_1, lower Ordovician.
The parameters (ratios) are interpreted in the footnote to Table 2.

Table 6
The fraction contributions of endmember oils to crude oil samples calculated by ALS-C.

No.	Well	Reservoir	Depth, m	EM1, %	EM2, %	EM3, %
1	Ln632	O	6452–6472	6	8	86
2	Lg392	O	6330–6350	1	64	36
3	Lg39	O	5861–5717	0	11	89
4	Lg352	O	5872–6110	0	30	70
5	Ln62	C	5565–5578	11	12	77
6	Ln635	O	5815–5842	0	32	68
7	Ln631(1)	O	5844–5884	0	25	75
8	Ln631(3)	O	5902–5990	0	19	81
9	Ln63(2)	O	5957–6071	34	0	66
10	Lg100-H1	O	5541–5605	0	33	67
11	Lg100	O	5431–5525	3	37	60
12	Lg101-4	O	5459–5490	0	36	64
13	Lg12	O	5407–5528	2	13	85
14	Lg16c	O	5468–5600	0	40	60
15	Lg17C	C	5245–5268	0	41	59
16	Lg17(o)	O	5464–5479	2	35	63
17	Ln51	O	5418–5550	20	17	63
18	Ln44	O	5283–5323	1	44	55
19	Ln46	O	6119–6144	10	33	57
20	Ln16	O	5585–5605	5	23	72
21	Lg4O1	O	5270–5296	5	20	76
22	Lg4O	O	5379–5397	6	34	60
23	Lg8	O	5145–5220	0	33	67
24	Ln8	O	5167–5230	0	34	66
25	Lg1	O	5210–5590	0	51	49
26	Lg202	O	5142–5146	4	28	68
27	Lg208	O	5330–5370	0	47	53
28	Ln18-1	O	5244–5350	14	11	75
29	Lg6c	O	5416–5430	0	35	64
30	Lg2-1	O	5421–5510	4	52	44
31	Lg2	O	5345–5431	4	47	50
32	Lg21	O	5043–5060	0	38	62
33	Lg201	O	5350–5353	4	42	54
34	Ln19(1)	O	5570–5585	8	11	81
35	Ln19(2)	O	5338–5360	10	9	81
36	Ln10(1)	O	5283–5343	0	49	51
37	Ln2-1c	O	5364–5458	2	60	37
38	Ln11	O	5278–5310	0	5	95
39	Lg3	C	5196–5270	2	25	72
40	Ln101	O	5049–5150	29	17	54
41	Ln1	O	5038–5052	0	10	90
42	Lg15	O	5726–5750	10	22	68
43	Lg15-1	O	5904–5954	0	17	83
44	Lg40	O	5339–5346	14	16	70
45	Lg903	O	5530–5568	16	3	81
46	S47	O	5344–5370	12	8	80
47	S65	O	/	10	7	84
48	Ha6c(1)	O	6731–6830	8	72	20
49	Ha6c(2)	O	6746–6830	5	68	28
50	Ha7	O	6622–6646	3	50	47
51	Ha8	O	6643–6680	2	36	62
52	Ha9	O	6598–6710	4	57	39
53	Ha11	O	6658–6748	0	46	54
54	Ha12	O	6694–6696	5	54	42
55	Ha13	O	6668–6800	0	43	57
56	Ha601	O	6598–6677	0	48	52
57	Ha701	O	6557–6618	3	84	13
58	HD23	O	6253–6440	8	18	74
59	YM2	O	5940–5953	2	10	88
60	YG2	O	6009–6070	4	7	89
61	Tz62	S	4052–4074	100	0	0

generated from Cambrian–Lower Ordovician source rocks in the early to peak oil generation stage. EM1 is a minor contributor to the mixed oils. It migrated into the Palaeozoic reservoirs during the late Caledonian orogeny and subsequently experienced two phases of mixing and biodegradation. EM2 is the secondary contributor to the mixed oils and its proportions are in the range 10–40% in most oils. It was generated in the early oil generation stage, filled the Palaeozoic reservoirs during the late Hercynian orogeny and experienced two phases of mixing and one stage of biodegradation. EM3 is the major contributor to most oils and its proportions are in the range 13–95%. It was generated in the late oil generation stage and migrated into the Palaeozoic reservoirs where it mixed with the previous residual mixtures during the late Yanshan to Himalayan orogeny. The final mixtures were not biodegraded further and are currently produced from the Palaeozoic reservoirs in the Tabei Uplift.

Acknowledgements

We are grateful to Drs. Kenneth E. Peters, Brian G. Rohrback and Erdem Idiz for critical reviews that significantly improved the quality of the manuscript. We thank Drs. Xiaowan Tao, Mei Li and Chao Liu for help in this study. The CNPC-CAS strategic cooperation project (Grant No. RIPED-2015-JS-255), NSFC (Grant Nos. 41273059 and 41173054), GIGCAS 135 project (Grant No. Y234021001) and Earmarked Fund of the State Key Laboratory of Organic Geochemistry (Grant No. sklog2012A02) are acknowledged for financial support. This is contribution No. IS-2216 from GIGCAS.

Appendix A. Supplementary data

Supplementary data associated with this article can be found, in the online version, at http://dx.doi.org/10.1016/j.orggeochem.2016.04.004.

Associate Editor—**Kenneth E Peters**

References

Arouri, K.R., McKirdy, D.M., 2005. The behaviour of aromatic hydrocarbons in artificial mixtures of Permian and Jurassic end-member oils: application to in-reservoir mixing in the Eromanga Basin, Australia. Organic Geochemistry 36, 105–115.

Cai, C., Zhang, C., Cai, L., Wu, G., Lei, J., Xu, Z., Li, K., Ma, A., Chen, L., 2009a. Origins of Palaeozoic oils in the Tarim Basin: evidence from sulfur isotopes and biomarkers. Chemical Geology 268, 197–210.

Cai, C., Li, K., Anlai, M., Zhang, C., Xu, Z., Worden, R.H., Wu, G., Zhang, B., Chen, L., 2009b. Distinguishing Cambrian from Upper Ordovician source rocks: evidence from sulfur isotopes and biomarkers in the Tarim Basin. Organic Geochemistry 40, 755–768.

Chang, X., Wang, T., Li, Q., Cheng, B., Tao, X., 2013. Geochemistry and possible origin of petroleum in Palaeozoic reservoirs from Halahatang Depression. Journal of Asian Earth Sciences 74, 129–141.

Connan, J., Cassau, A.M., 1980. Properties of gases and petroleum liquids derived from terrestrial kerogen at various maturation levels. Geochimica et Cosmochimica Acta 44, 1–23.

Dzou, L.I.P., Noble, R.A., Senftle, J.T., 1995. Maturation effects on absolute biomarker concentration in a suite of coals and associated vitrinite concentrates. Organic Geochemistry 23, 681–697.

Guo, J., Chen, J., Wang, T., Ye, Z., Zhou, X., Shi, S., 2008. New progress in studying Cambrian source rock of Tarim Basin. Acta Sedimentologica Sinica 26 (3), 518–524 (in Chinese with English abstract).

Hanson, A.D., Zhang, S.C., Moldowan, J.M., Liang, D.G., Zhang, B.M., 2000. Molecular organic geochemistry of the Tarim Basin, Northwest China. American Association of Petroleum Geologists Bulletin 84, 1109–1128.

Hughes, W.B., Holba, A.G., Dzou, L.I.P., 1995. The ratios of dibenzothiophene to phenanthrene and pristane to phytane as indicators of depositional environment and lithology of petroleum source rocks. Geochimica et Cosmochimica Acta 59, 3581–3598.

Jia, W., Peng, P., Xiao, Z., 2008. Carbon isotopic compositions of 1,2,3,4-tetramethylbenzene in marine oil asphaltenes from the Tarim Basin: evidence for the source formed in a strongly reducing environment. Science in China Series D 51, 509–514.

Jia, W., Peng, P., Yu, C., Xiao, Z., 2010. Molecular and isotopic compositions of bitumens in Silurian tar sands from the Tarim Basin, NW China: characterizing biodegradation and hydrocarbon charging in an old composite basin. Marine and Petroleum Geology 27, 13–25.

Jia, W., Wang, Q., Peng, P.A., Xiao, Z., Li, B., 2013. Isotopic compositions and biomarkers in crude oils from the Tarim Basin: oil maturity and oil mixing. Organic Geochemistry 57, 95–106.

Li, D., Liang, D., Jia, C., Wang, G., Wu, Q., He, D., 1996. Hydrocarbons accumulations in the Tarim Basin, China. American Association of Petroleum Geologists Bulletin 80, 1587–1603.

Li, M., Xiao, Z., Snowdon, L., Lin, R., Wang, P., Hou, D., Zhang, L., Zhang, S., Liang, D., 2000. Migrated hydrocarbons in outcrop samples: revised petroleum exploration directions in the Tarim Basin. Organic Geochemistry 31, 599–603.
Li, S., Pang, X., Jin, Z., Yang, H., Xiao, Z., Gu, Q., Zhang, B., 2010. Petroleum source in the Tazhong Uplift, Tarim Basin: new insights from geochemical and fluid inclusion data. Organic Geochemistry 41, 531–553.
Li, S., Shi, Q., Pang, X., Zhang, B., Zhang, H., 2012. Origin of the unusually high dibenzothiophene oils in Tazhong-4 oilfield of Tarim Basin and its implication in deep petroleum exploration. Organic Geochemistry 48, 56–80.
Li, S., Amrani, A., Pang, X., Yang, H., Said-Ahmad, W., Zhang, B., Pang, Q., 2015. Origin and quantitative source assessment of deep oils in the Tazhong Uplift, Tarim Basin. Organic Geochemistry 78, 1–22.
Liang, D., Zhang, S., Zhang, B., Wang, F., 2000. Understanding of marine oil generation in China based on Tarim Basin. Earth Science Frontiers 7 (4), 534–547 (in Chinese with English abstract).
Lu, Y., Xiao, Z., Gu, Q., Zhang, Q., 2008. Geochemical characteristics and accumulation of marine oil and gas around Halahatang depression, Tarim Basin, China. Science in China, Series D: Earth Sciences 51 (Suppl. 1), 195–206.
Meng, S., 2010. Investigation on Marine Oil and Gas Accumulation in the Carboniferous Reservoirs in the Northern Tarim Basin (Master degree dissertation). China University of Geoscience, Beijing.
Pan, C., Liu, D., 2009. Molecular correlation of free oil, adsorbed oil and inclusion oil of reservoir rocks in the Tazhong Uplift of the Tarim Basin, China. Organic Geochemistry 40, 387–399.
Peters, K.E., Moldowan, J.M., 1991. Effects of source, thermal maturity, and biodegradation on the distribution and isomerization of homohopanes in petroleum. Organic Geochemistry 17, 47–61.
Peters, K.E., Moldowan, J.M., McCaffrey, M.A., Fago, F.J., 1996. Selective biodegradation of extended hopanes to 25-norhopanes in petroleum reservoirs. Insights from molecular mechanics. Organic Geochemistry 24, 765–783.
Peters, K.E., Walters, C.C., Moldowan, J.M., 2005. The Biomarker Guide, second ed. Cambridge University Press, Cambridge.
Peters, K.E., Scott Ramos, L., Zumberge, J.E., Valin, Z.C., Scotese, C.R., Gautier, D.L., 2007. Circum-Arctic petroleum systems identified using decision-tree chemometrics. American Association of Petroleum Geologists Bulletin 91, 877–913.
Peters, K.E., Hostettler, F.D., Lorenson, T.D., Rosenbauer, R.J., 2008a. Families of Miocene Monterey crude oil, seep, and tarball samples, coastal California. American Association of Petroleum Geologists Bulletin 92, 1131–1152.
Peters, K.E., Scott Ramos, L., Zumberge, J.E., Valin, Z.C., Bird, K.J., 2008b. De-convoluting mixed crude oil in Prudhoe Bay Field, North Slope, Alaska. Organic Geochemistry 39, 623–645.
Peters, K.E., Coutrot, D., Nouvelle, X., Ramos, L.S., Rohrback, B.G., Magoon, L.B., Zumberge, J.E., 2013. Chemometric differentiation of crude oil families in the San Joaquin Basin, California. American Association of Petroleum Geologists Bulletin 97, 103–143.
Radke, M., Welte, D.H., 1983. The methylphenanthrene index (MPI): a maturity parameter based on aromatic hydrocarbons. In: Bjøroy, M., Albrecht, P., Cornford, C., de Groot, K., Eglinton, G., Galimov, E., Leythaeuser, D., Pelet, R., Rullotter, J., Speers, G. (Eds.), Advances in Organic Geochemistry 1981. Wiley, Chichester, pp. 504–512.
Radke, M., Welte, D.H., Willsch, H., 1986. Maturity parameters based on aromatic hydrocarbons: influence of the organic matter type. Organic Geochemistry 10, 51–63.
Sun, Y., Xu, S., Lu, H., Cai, P., 2003. Source facies of the Paleozoic petroleum systems in the Tabei uplift, Tarim Basin, NW China. Organic Geochemistry 34, 629–634.
Tao, G., Qin, J., Tun, G., Zhang, M., Fu, X., Lou, Z., 2010. Comparative study of geochemistry and multivariate data analysis on mixed oils accumulated in Ordovician reservoir in Tahe Oilfield, Tarim Basin, NW China. Geological Journal of China Universities 16 (4), 527–538 (in Chinese with English abstract).
Tian, Y., 2013. Geochemical Quantification of Marine Mixed Oils Tazhong and Tabei Uplift, Tarim Basin, NW China (PhD dissertation). Guangzhou Institute of Geochemistry, Chinese Academy of Science, Guangzhou.
Tian, Y., Yang, C., Liao, Z., Zhang, H., 2012a. Geochemical quantification of mixed marine oils from Tazhong area of Tarim Basin, NW China. Journal of Petroleum Science and Engineering 90–91, 96–106.
Tian, Y., Zhao, J., Yang, C., Liao, Z., Zhang, L., Zhang, H., 2012b. Multiple-sourced features of marine oils in the Tarim Basin, NW China – geochemical evidence from occluded hydrocarbons inside asphaltenes. Journal of Asian Earth Sciences 54–55, 174–181.
Wang, T.-G., Wang, C., He, F., Wang, J., Zhu, D., Wang, C., Xie, M., 2004. Determination of double filling ratio of mixed crude oils in the Ordovician oil reservoir, Tahe Oilfield. Petroleum Geology & Experiment 26 (1), 74–79 (in Chinese with English abstract).
Wang, T.-G., He, F., Wang, C., Zhang, W., Wang, J., 2008. Oil filling history of the Ordovician oil reservoir in the major part of the Tahe Oilfield, Tarim Basin, NW China. Organic Geochemistry 39, 1637–1646.
Xiao, Z., Lu, Y., Sang, H., Pan, Z., Li, Y., 2005. A typical Cambrian oil reservoir: origin of oil reservoir in well TZ62, Tarim Basin. Geochimica 34 (2), 155–160 (in Chinese with English abstract).
Yang, J., Huang, H., Zhang, S., Chen, F., 2003. Semi-quantitative evaluation of mixed oil in northern uplift of the Tarim Basin. Geochimica (Beijing) 32, 105–111 (in Chinese with English abstract).
Yu, S., Pan, C., Wang, J., Jin, X., Jiang, L., Liu, D., Lü, X., Qin, J., Qian, Y., Ding, Y., Chen, H., 2011. Molecular correlation of crude oils and oil components from reservoir rocks in the Tazhong and Tabei uplifts of the Tarim Basin, China. Organic Geochemistry 42, 1241–1262.
Zhai, X., Gu, Y., Qian, Y., Jia, C., Wang, J., Lin, J., 2007. Geochemical characteristics of the Cambrian oil and gas in well Tashen 1, the Tarim Basin. Petroleum Geology & Experiment 29 (4), 329–333 (in Chinese with English abstract).
Zhan, Z.-W., Zou, Y.-R., Shi, J.-T., Sun, J.-N., Peng, P.A., 2016. Unmixing of mixed oil using chemometrics. Organic Geochemistry 92, 1–15.
Zhang, S., 2000. The migration fractionation: an important mechanism in the formation of condensate and waxy oil. Chinese Science Bulletin 45, 1341–1344.
Zhang, S., Huang, H., 2005. Geochemistry of Palaeozoic marine petroleum from the Tarim Basin, NW China: Part 1. Oil family classification. Organic Geochemistry 36, 1204–1214.
Zhang, S., Hanson, A.D., Moldowan, J.M., Graham, S.A., Liang, D., Chang, E., Fago, F., 2000. Paleozoic oil-source rock correlations in the Tarim Basin, NW China. Organic Geochemistry 31, 273–286.
Zhang, S., Liang, D., Zhang, B., 2004. Hydrocarbon Generation from Marine Source Rocks of Tarim Basin. Petroleum Industry Press, Beijing (in Chinese).
Zhang, S., Huang, H., Xiao, Z., Liang, D., 2005. Geochemistry of Palaeozoic marine petroleum from the Tarim Basin, NW China. Part 2: maturity assessment. Organic Geochemistry 36, 1215–1225.
Zhang, Z., Liu, W., Wang, Z., Zheng, J., Wang, Q., Chen, G., 2008. Vertical distribution characteristics and its Geological Significance for carbon isotopic composition of oils and its group components of deep marine oil reservoirs in Tabei Uplift, Tarim Basin. Acta Sedimentologica Sinica 26 (4), 709–714 (in Chinese with English abstract).
Zhang, S., Su, J., Wang, X., Zhu, G., Yang, H., Liu, K., Li, Z., 2011. Geochemistry of Palaeozoic marine petroleum from the Tarim Basin, NW China. Part 3: thermal cracking of liquid hydrocarbons and gas washing as the major mechanisms for deep gas condensate accumulations. Organic Geochemistry 42, 1394–1410.
Zhang, S., Huang, H., Su, J., Zhu, G., Wang, X., Larter, S., 2014. Geochemistry of Paleozoic marine oils from the Tarim Basin, NW China. Part 4: paleobiodegradation and oil charge mixing. Organic Geochemistry 67, 41–57.
Zhang, S., Huang, H., Su, J., Liu, M., Wang, X., Hu, J., 2015. Geochemistry of Paleozoic marine petroleum from the Tarim Basin, NW China: Part 5. Effect of maturation, TSR and mixing on the occurrence and distribution of alkyldibenzothiophenes. Organic Geochemistry 86, 5–18.
Zhu, G., Zhang, S., Su, J., Huang, H., Yang, H., Gu, L., Zhang, B., Zhu, Y., 2012. The occurrence of ultra-deep heavy oils in the Tabei Uplift of the Tarim Basin, NW China. Organic Geochemistry 52, 88–102.
Zhu, G., Zhang, S., Su, J., Zhang, B., Yang, H., Zhu, Y., Gu, L., 2013. Alteration and multi-stage accumulation of oil and gas in the Ordovician of the Tabei Uplift, Tarim Basin, NW China: implications for genetic origin of the diverse hydrocarbons. Marine and Petroleum Geology 46, 234–250.
Zhu, C., Yan, H., Yun, L., Han, Q., Ma, H., 2014a. Characteristics of Cambrian source rocks in well XH1, Shaya Uplift, Tarim Basin. Petroleum Geology & Experiment 36 (5), 626–632 (in Chinese with English abstract).
Zhu, G., Zhang, B., Yang, H., Su, J., Liu, K., Zhu, Y., 2014b. Secondary alteration to ancient oil reservoirs by late gas filling in the Tazhong area, Tarim Basin. Journal of Petroleum Science and Engineering 122, 240–256.